ADVANCED INSTRUMENTATION CONCEPTS AND THEIR APPLICATION TO NUCLEAR POWER PLANTS

by

RALPH T. SOULE

B.S. Electrical Engineering, U.S Naval Academy (1982)

SUBMITTED TO THE DEPARTMENTS OF

NUCLEAR ENGINEERING
and
ELECTRICAL ENGINEERING AND COMPUTER SCIENCE

IN PARTIAL FULFILLMENT OF THE REQUIREMENTS FOR THE DEGREES OF

MASTER OF SCIENCE IN NUCLEAR ENGINEERING

and

MASTER OF SCIENCE IN ELECTRICAL ENGINEERING

at the
MASSACHUSETTS INSTITUTE OF TECHNOLOGY

May 1991

ADVANCED INSTRUMENTATION CONCEPTS AND THEIR APPLICATION TO NUCLEAR POWER PLANTS

by

RALPH T. SOULE

B.S. Electrical Engineering, U.S Naval Academy
(1982)

SUBMITTED TO THE DEPARTMENTS OF

NUCLEAR ENGINEERING
and
ELECTRICAL ENGINEERING AND COMPUTER SCIENCE

IN PARTIAL FULFILLMENT OF THE REQUIREMENTS
FOR THE DEGREES OF

MASTER OF SCIENCE IN NUCLEAR ENGINEERING

and

MASTER OF SCIENCE IN ELECTRICAL ENGINEERING

at the
MASSACHUSETTS INSTITUTE OF TECHNOLOGY

May 1991

Signature of Author: _____
Department of Nuclear Engineering
May 1991

Certified by: _____
John E. Meyer
Professor Of Nuclear Engineering
Thesis Supervisor

Certified by: _____
Stephen K. Burns
Professor Of Electrical Engineering
Thesis Reader

Accepted by: _____
Allan F. Henry
Chairman, Department Committee on Graduate Students

ADVANCED INSTRUMENTATION CONCEPTS AND THEIR APPLICATION TO NUCLEAR POWER PLANTS

by

RALPH T. SOULE

Submitted to the Departments of Nuclear Engineering and Electrical Engineering And Computer Science in partial fulfillment of the requirements for the degrees of Master of Science in Nuclear Engineering and Master of Science in Electrical Engineering

ABSTRACT

The characteristics of computer based instrumentation, or smart instruments, are investigated. Computer based instruments are distinguished by their ability to include a more complex model of the physical processes influencing the desired measurement than is possible with conventional instrument. Smart instrumentation is described with emphasis on illustrating its ability to improve data collection, storage, display, and evaluation. The application considerations of redundancy, consistency, noise, and filtering are also addressed.

As an application example, a smart instrument for measuring steam generator water level in a pressurized water reactor is designed. A model, accounting for the important processes affecting level measurement is developed. An error exists in the computation the fluid shear stresses, but the model calculations remain illustrative of those pertinent to smart instrument design. The model is stable for both steady state and transient conditions, but there are restrictions on the rate of the transient. Simulated level data is used to compare a simplified level instrument with the smart level instrument. The smart instrument is more accurate, but not by more than one percent. Methods that could be used by a smart instrument to recover from operation outside its model assumptions are discussed. Finally, recommendations are made for future work.

Thesis Supervisor: John E. Meyer
Title: Professor Of Nuclear Engineering

Acknowledgements

I wish to express my gratitude to Professor Meyer, my thesis advisor, for his patient assistance and guidance provided throughout the preparation of this report. I am also grateful for the advice and assistance I received from Professor Burns, my thesis reader. Thanks also to Erv LaForge for the administrative assistance he provided. Finally, I want to thank my family, Pamela and Bryan, for the enormous patience and support they provided while I completed my research.

Table of Contents

Table Of Contents (cont'd)

List of Figures

List of Tables

List of Symbols

The units, if any, of each symbol are shown in [] and the first equation which uses the symbol is denoted by the number in ()

- A ▲ the total cross sectional area of the drain pipe [m^2] (4)
- A_v ▲ cross sectional area of the vapor phase [m^2] (28)
- A_ℓ ▲ cross sectional area of the liquid phase [m^2] (15)
- a_ℓ ▲ energy or coriolis coefficient (9)
- $C_{v,\ell}$ = Constant in friction factor correlation (value used = .184), based on Darcy - Weisbach correlation
- c_p ▲ specific heat capacity of liquid water [J/kg-K] (52)
- D_t ▲ diameter of the drain pipe [m] (9)
- g ▲ acceleration due to gravity [m/sec^2] (1)
- H ▲ height of water in the reference leg [m] (1)
- H_c ▲ the total mass-enthalpy product in the condensing pot [J] (5)
- H_ℓ ▲ the enthalpy of the liquid leaving the condensing pot [J/kg] (5)
- H_v ▲ the enthalpy of the vapor entering the condensing pot from the steam generator [J/kg] (5)
- h_{air} ▲ film heat transfer coefficient for air in the reactor building [W/m^2-K] (42)
- h_w ▲ liquid height at the weir [m] (36)
- h_{fg} ▲ latent heat of vaporization [J/kg] (43)
- h_{stm} ▲ film heat transfer coefficient for the water vapor condensing on the inside surface of the condensing pot [W/m^2-K] (42)

List of Symbols (cont'd)

j_{fw}	▲	superficial liquid velocity at the weir [m/sec] (9)
j_v	▲	superficial vapor velocity of the vapor entering the condensing pot from the steam generator [m/s] (4)
k_{st}	▲	thermal conductivity of condensing pot [W/m] (42)
k	▲	thermal conductivity of water [W/m-K] (43)
L	▲	downcomer level [m] (1)
L_c	▲	wetted length of condensing pot [m] (42)
L_s	▲	significant length of condensing pot [m] (44)
L_t	▲	the total length of the drain pipe [m] (15)
M_c	▲	mass of water in the condensing pot [kg] (4)
M_t	▲	total mass of water in the drain line [kg] (8)
$\dot{m}_{dc}$	▲	mass flow rate of water in downcomer [kg/sec] (52)
$\dot{m}_{fw}$	▲	mass flow rate of feedwater [kg/sec] (52)
$\dot{m}_l$	▲	mass flow rate of liquid condensing in the condensate pot [kg/sec] (45)
$\dot{m}_w$	▲	the mass flow rate of liquid leaving the condensing pot in the weir [kg/sec] (4)
n	=	exponent in friction factor correlation (value used was .2)
Nu_l	▲	Nusselt number (43)
P_A	▲	pressure on reference leg side of differential pressure cell [Pa] (1)
P_B	▲	pressure on downcomer side of differential

pressure cell [Pa] (1)

p_c ▲ pressure in condensing pot [Pa] (1)

p_{sg} ▲ pressure of vapor in steam generator adjacent to the drain pipe [Pa] (1)

$\dot{Q}$ ▲ the heat loss from the condensing pot to ambient [W] (5)

$R_{t_{stm}}$ ▲ thermal resistance of the condensing steam film (46)

r_{in} ▲ inner radius of the condensing pot [m] (42)

r_{out} ▲ outer radius of condensing pot [m] (42)

S_ℓ ▲ wetted perimeter of liquid phase [m] (29)

S_i ▲ interfacial wetted perimeter [m] (28)

S_v ▲ wetted perimeter of vapor phase [m] (28)

T_{dc} ▲ temperature of downcomer water [°C] (52)

T_{fw} ▲ temperature of feedwater [°C] (52)

T_{in} ▲ temperature of inner surface of condensing pot [°C] (43)

T_{sat} ▲ saturation temperature of generator pressure [°C] (52)

T_{stm} ▲ temperature corresponding to saturation pressure in condensing pot [°C] (43)

V_c ▲ the total volume of the condensing pot [m^3] (5)

Greek Letters

α_b ▲ vapor fraction at the boundary between the condensing pot and the top of the drain pipe (9)

ΔP ▲ pressure difference (reference leg

pressure minus variable leg pressure) [Pa] (1)

θ ▲ angle of elevation of drain pipe from horizontal [radians] (9)

μ ▲ dynamic viscosity of water [kg/m-sec] (43)

$\mu_{v,\ell}$ ▲ dynamic viscosity of vapor and liquid in condensing pot [kg/m-sec]

ρ_{dc} ▲ density of fluid in the downcomer [kg/m^3] (1)

ρ_ℓ ▲ density of the liquid leaving the condensing pot [kg/m^3] (6)

ρ_r ▲ density of fluid in reference leg [kg/m^3] (1)

ρ_v ▲ density of vapor in the steam generator [kg/m^3] (1)

τ_i ▲ interfacial shear stress [Pa] (28)

$\tau_{w\ell}$ ▲ wall to liquid phase shear stress [Pa] (29)

τ_{wv} ▲ wall to vapor phase shear stress [Pa] (28)

Introduction

Chapter 1

The objective of this research is to suggest a method for the application of microcomputer based instrumentation to nuclear power plants. The specific instrument illustrated is for a steam generator level measurement, but the basic steps of physical process selection, variable identification, model creation, and integration of the process model with signal validation are applicable to any important plant parameter. A procedure to implement a smart instrument is suggested. A model was developed to include important physical features of the level instrument process. This model was simplified and used as a basis for a computer based steam generator level instrument. Although the model is based on fundamental properties and relationships, its accuracy and the limits of its application cannot be established fully until comparisons can be mad with experimental data.

1.1 Purpose of Simulation

The optimum method for evaluation of the proposed steam generator level instrument would be to compare the outputs of a conventional level measurement device and the measurements of a microprocessor-based level instrument given identical inputs from an actual steam generator. However, since the concept is still being developed, the more prudent approach is to perform extensive lab tests prior to implementation of this smart instrument on an actual power plant. To evaluate the potential effectiveness

of the proposed smart level instrument, typical steam generator level pressure and power relations are established to provide simulated "measured" data for the physical input variables that the smart level instrument would require and for a simulated "known" level signal for the basis of comparison. While it is somewhat artificial to base measurement results upon simulated input data, this procedure does provide a qualitative and quantitative sense for the capabilities that a smart instrument would have and serves as a first step for future research.

1.2 Smart Instrumentation

In the context of this thesis, a smart instrument is one that includes a detailed model of the physical process being measured to enhance both the reliability and accuracy of the instrument. In addition, the model can give the instrument the capability to infer quantities that are not actually measured. For example, a temperature sensor could be used to control a heating coil for bringing a solution in a beaker to a desired temperature. A smart temperature sensor could detect the absence of the solution from the beaker and protect the heating coil by noting whether the rate of the temperature increase just after energizing the heater was consistent with that expected when the solution was present, and de-energize the heating coil appropriately.

1.3 Background

Accurate indication and measurement of plant variables are required for safe operation of nuclear reactors. Information recorded by instruments is used to advise plant supervisors about the operability and reliable operation of nearly all plant components, to provide inputs to protection

systems, and to furnish input to automatic control systems. In the past, instrumentation was not sophisticated enough to enhance accuracy by using information about the process being modeled; often attempts were made to design instrumentation resistant to sources of signal degradation, but the design was usually based on worst case or very simplified assumptions about sources of measurement error. In addition, conservative estimates are generally made to account for the tendency of the transducer and associated circuitry to exhibit characteristics varying with time so that regular calibrations could be done prior to receiving erroneous readings. Recent attempts to integrate microcomputers into plant instrumentation and to employ signal validation techniques have illustrated the potential benefits of more sophisticated instruments (references S1 and M2). Signal validation increases information reliability by combining information from redundant sensors and a detailed knowledge of the dynamics of plant systems. Detection of faulty sensor operation, a highly desirable function, is an important component of signal validation that can be accomplished by high speed comparison of redundant sensors in conjunction with knowledge of prior sensor data.

The premise of this research is that microcomputers, when included as integral components of plant sensors, can perform the functions of signal measurement, validation, and fault detection to enhance instrument reliability and accuracy. Using microcomputers within each sensor enables one to program into the instrument an accurate model of the physically pertinent variables and their relationships which can enhance the accuracy of the instrument as well as provide a localized determination of the quality of data presented, also known as distributed processing. This information can be used to alert the operator to the onset

of conditions that could produce erroneous readings as well as extending the time between required instrument calibrations. In addition, redundancy and consistency checking of measured data can be done locally by a group of smart instruments.

1.4 Motivation

Accurate steam generator water level information is essential for safe operation of pressurized water reactors (PWR). The steam generators are the source of the steam used to drive the power turbines and are the heat sink for the primary coolant that flows through the reactor. Maintaining steam generator water level below the upper limit of the designated operating band is necessary to prevent carryover of liquid droplets to the turbines, which could cause severe turbine blade erosion and possibly tremendous damage to the turbine itself. Steam generator water level must not be allowed to drop below the lower limit of the designed band since this could uncover the generator U-tubes, resulting in inadequate heat removal from the reactor and significant thermal stresses to the U-tubes themselves, possibly leading to their premature failure. Clearly, it is desirable to enhance the reliability of the level information provided to plant operators and to the automatic control systems responsible for maintaining generator water level within normal bounds. Using a computer to record plant data is not a new concept, but the smart instrument would be able to interpret the measured data as well and by placing the computing resource as close as possible to the variables being measured, higher level computers utilized in the plant can be freed to perform integrating roles on the basis of input information of improved quality.

tubes by a tube bundle wrapper which forces the feed water through the downcomer region, so the feed water can be pre-heated by the hot water falling from the moisture separators. The feedwater flows up through the U-tube

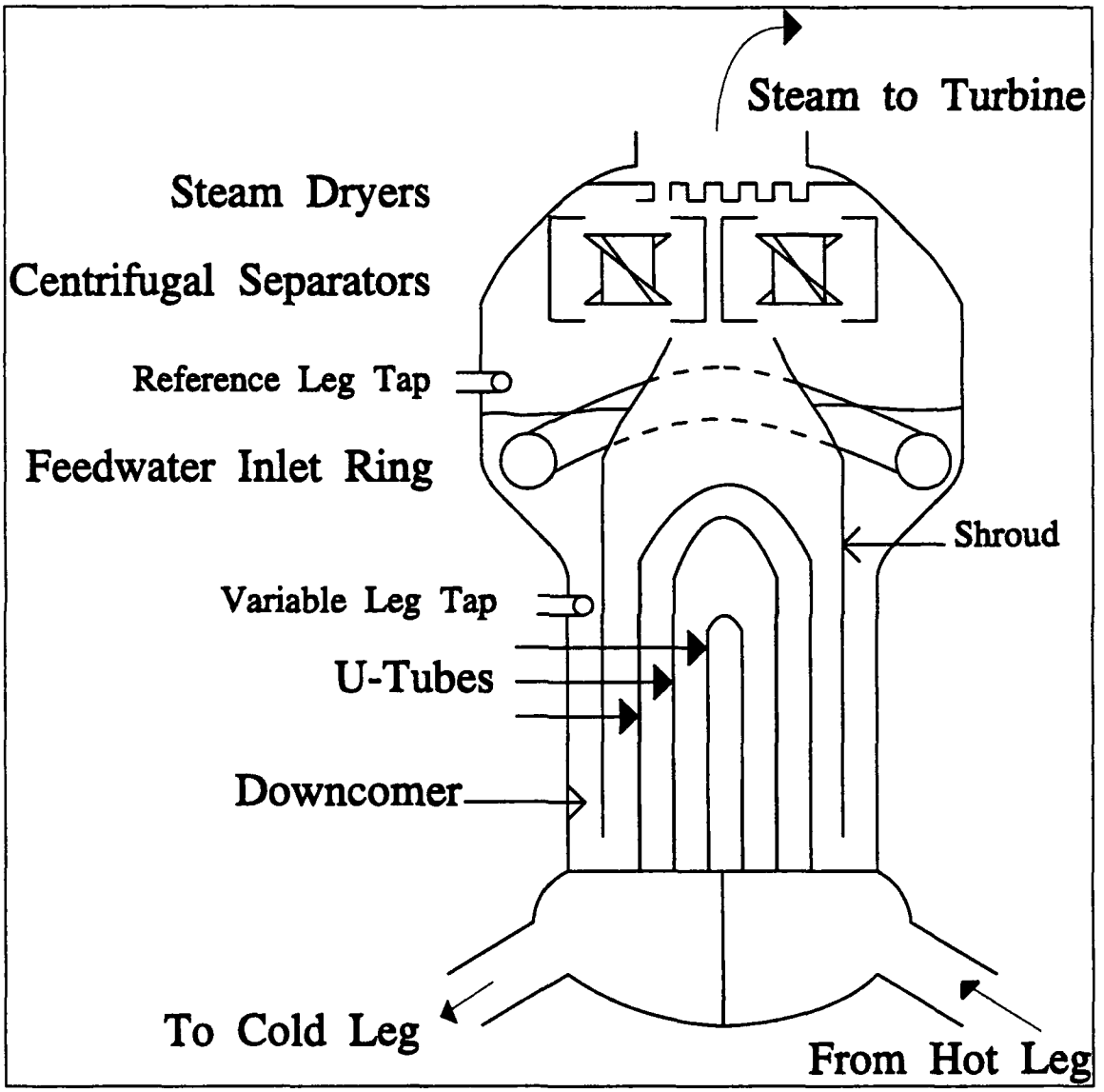

Figure 1: Steam Generator Internals

region where it is heated and transformed to steam because of the lower pressure of the secondary loop. The two phase

Chapter 2

Steam Generator Description

Each primary loop in a Pressurized Water Reactor contains a steam generator, important and very large (typically 20 meters high, 4 meters in diameter) components which are used to transfer heat from a primary coolant, flowing through the reactor core at high pressure, to a secondary coolant, which does not flow through the core, to produce the steam necessary to drive turbo generators.

2.1 Steam Generator Internal Description

There are three basic steam generator designs: vertical U-tube, once-through, and the horizontal U-tube. Since the vertical U-tube generator (Figure 1) is the most widely used, only its operation and level sensing configuration will be discussed here. The steam generator is a heat exchanger that enables the primary coolant to boil the secondary coolant without allowing the two fluids to mix. The hot, primary coolant just exited from the reactor vessel enters the steam generator at the inlet plenum, located at the lower end of the steam generator, passes upward then downward through the U-tubes, enters the exit plenum and returns to the cold leg reactor piping. Mixing of the inlet and outlet plenums is prevented by an isolation plate separating the two. Condensed steam, known as condensate or feedwater, enters the steam generator via an annular piping arrangement inside the generator called the feedwater inlet ring. Cold feedwater is prevented from impinging upon the

mixture passes upward from the U-tube region through the moisture separators, which allow the steam to pass but cause virtually all of the entrained liquid to fall back within the steam generator and mix with incoming feedwater, as mentioned above.

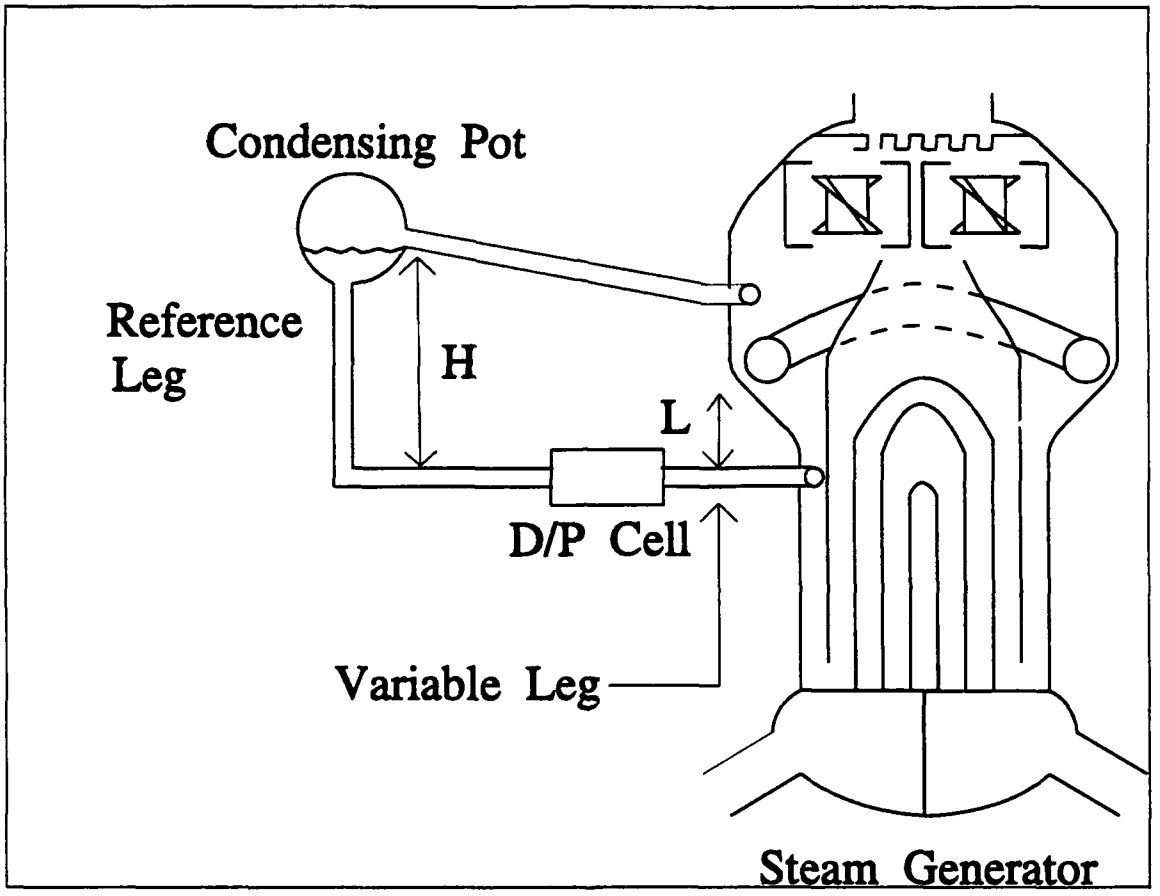

Figure 2: Steam Generator Level Sensing System

2.2 Level Sensing

Figure 2 shows a schematic representation of a typical steam generator level remote sensing system. It is analogous to the method used to measure core water level in a boiling water reactor (BWR) and the method used to measure the pressurizer level in a pressurized water reactor (PWR)

plant. The system depicted is sometimes called a cold reference leg system because the reference leg piping is not heated or insulated so it assumes the temperature of the ambient air in the reactor building. The downcomer level, the level in the area between the tube sheet wrapper and the generator vessel, is the variable actually measured and is considered the generator water level. That level is more easily measured and the two phase boiling process in the tube bundle region makes the level there ill-defined. As shown in Figure 2, an upper tap in the steam space is connected to a condensing pot and a reference leg. A lower tap in the liquid space is connected to a variable leg. The pressure difference, ΔP, between the reference and variable legs is measured by a differential pressure cell. The liquid level L may be calculated under the following assumptions:

(1) the fluid densities in the reference and variable legs are known,
(2) the liquid and vapor are separated, with liquid at the bottom and vapor at the top,
(3) the reference leg is completely filled with liquid to a known height,
(4) the density of the reference leg is constant, and
(5) there are no velocity dependent contributions to the pressure differences.

Figure 3 shows a schematic of the differential pressure cell arrangement, simplified to show just the details associated with the variable and reference legs. Based on figure 3, the differential pressure is approximately:

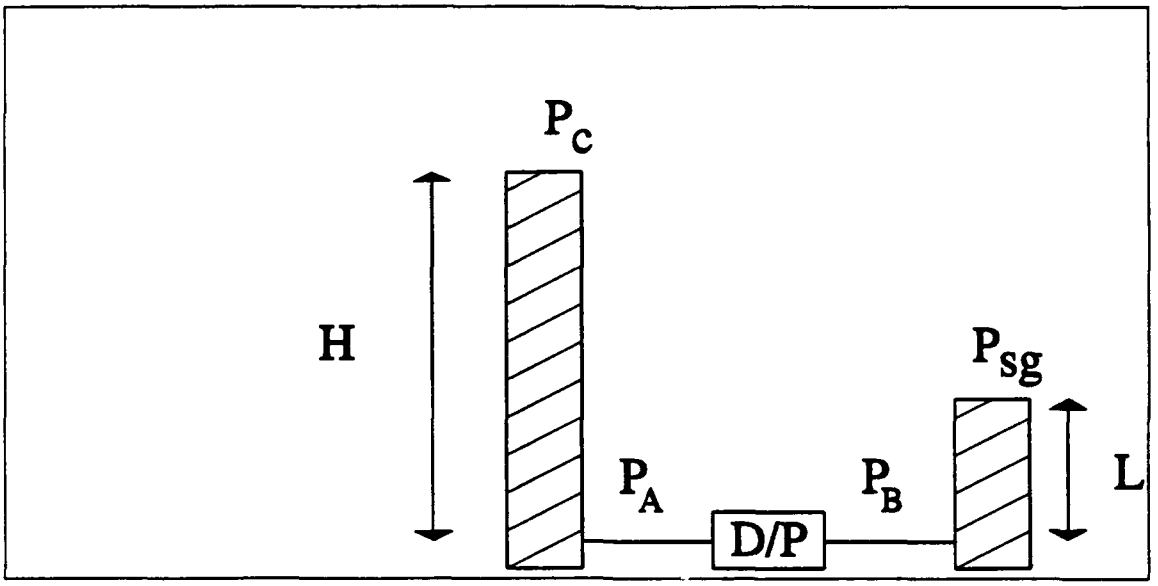

Figure 3: Differential Pressure Cell

$$P_A - P_B = \Delta P = (p_c - p_{sg}) + \rho_r H g - \rho_{dc} L g - \rho_v g (H - L) \quad (1)$$

and so the level is:

$$L = \frac{(p_c - p_{sg}) - \Delta P}{(\rho_{dc} - \rho_v) g} + \left(\frac{\rho_r - \rho_v}{\rho_{dc} - \rho_v} \right) H \quad (2)$$

where:

p_c	▲	pressure in condensing pot;
p_{sg}	▲	pressure in steam generator;
ρ_r	▲	density of fluid in reference leg;
ρ_{dc}	▲	density of fluid in the downcomer;
ρ_v	▲	density of vapor in the steam generator;
g	▲	acceleration due to gravity;
H	▲	height of water in the reference leg; and
L	▲	downcomer level.

Note that the level calculated by equation (2) is approximate since the height difference between the level of liquid in the condensing pot and the reference leg tap on

the steam generator is neglected. Otherwise, the numerator of the second term on the right hand side of equation (2) would be $(\rho_r H - \rho_v H_{tt})$ where H_{tt} is the vertical distance between the reference and variable leg taps on the side of the steam generator. Since ρ_r is so much larger than ρ_v, this approximation introduces little error.

2.3 Limitations of Conventional Level Sensing

Generally, the assumptions used for level measurements and noted above are valid and equation (1) provides a good estimate of steam generator level during normal operations. However, severe transients involving rapid depressurizations such as a generator steam leak could lower the pressure above the reference leg enough to cause flashing in the reference leg, violating assumption 3. Variations in the temperature of the reactor building will affect the rate of condensation in the condensing pot and the average density of the liquid in the reference leg. Generally, reactor building temperature is moderately related to time at power the power level of the reactor, and the outdoor temperature. In addition, a casualty such as a steam leak from the generator or a primary coolant leak could alter reactor building temperature enough to make assumption 4 invalid. The diameter of the piping chosen for the condensing pot drain line is also an important consideration. If the piping is not large enough to accommodate the flow of condensing liquid from the condensing pot during worst case conditions, the pipe may become filled with liquid, resulting in a decrease in effective reference leg height as the water level in the condensing pot rises above the drain line piping connection to the condensing pot. This condition violates assumption 4. There have been well-studied examples of this phenomenon actually occurring.

Finally, the steam that flows from the steam generator to the condensing pot and condenses does so because the condensing pot is uninsulated, but it would not be accurate to describe the condensation as taking place at reactor building ambient temperature. Contact between the inner surface of the condensing pot material and the steam from the steam generator no doubt elevates the average temperature of the condensing pot surface above reactor building ambient temperature. Still, the portions of the reference leg piping in the vicinity of the differential pressure cell are most nearly at ambient for the reactor building. Clearly, assumption 4 is not really accurate and the density of the reference leg varies along the length of the reference leg piping.

Chapter 3

Smart Instruments

A smart instrument is an electronic device, possessing memory and controlled by a microcomputer, used to measure some plant variable. Its computational and decision making capabilities, the salient features distinguishing smart from conventional instruments, enable the designer to integrate within the instrument a model of the physical process affecting the parameter being measured. To implement a smart instrument, the designer must choose an appropriate model and consider the roles of measurement consistency, data redundancy, and filtering. Smart instruments have many potential advantages over conventional instrumentation, but there are some tradeoffs to be considered as well

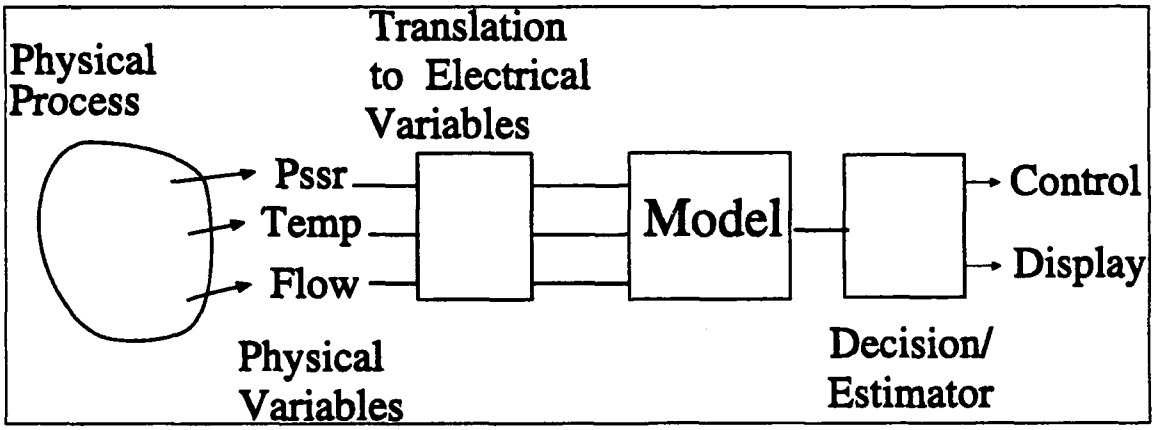

Figure 4: Smart Instrument Block Diagram

3.1 Model

Figure 4 shows a block diagram of a typical smart

instrument. It takes its inputs in the form of physical variables from some actual process and translates these natural phenomena into electrical variables like voltage or current. Conventional instruments process a transducer output signal in accordance with pre-determined assumptions selected by the designer. The processed transducer data is routed to a meter face and possible also connected to a data recording computer. While this has been a generally satisfactory method for presenting plant variable information to operators, it has two drawbacks. First, the burden of evaluating the consistency and accuracy of the data presented is entirely upon the operator. This context evaluation burden is not onerous when the total number of variables that the operator has to monitor are small, but it becomes considerably more difficult in the control room of a commercial power reactor having thousands of instruments and potentially hundreds of alarms to monitor.

Detecting instrument or transducer failure is especially complicated when the instrument continues to display a normal reading although its ability to respond at the extremes of its range might be severely degraded. The second limitation of conventional instruments is that they are only accurate as long as the design assumptions remain valid. The microcomputer controlling the smart instrument enables the designer to program into the instrument an "understanding" of the numerical characteristics of the system being measured. The complexity and accuracy of the model chosen for inclusion into the smart instrument is an important consideration. The primary benefit of a good model is that it enables the instrument itself to monitor measurement results and alert the operator if the data received from the sensors is not consistent with either: redundant transducers measuring the same variables or with other sensor information that can be fed to the smart

instrument. Judicious choice of the parameters to be monitored by the instrument and included into the computational model is essential. Selecting too few parameters and an oversimplified model risks realizing only a marginal improvement over existing instrumentation while an exceptionally complicated model that requires numerous interconnections with other sensors would require an enormously powerful computation engine that might dwarf the size of the original instrument, posing considerable debugging and robustness challenges.

3.2 Data Collection

It is important to establish some confidence that the data collected by the smart instrument is reliable. The important issues are: consistency of the detected signals with previous signals from the same transducer, comparison of the detected signals with current redundant signals, and filtering the detected signal to reduce the influence of electronic or process noise.

3.2.1 Consistency

It is desirable that the smart instrument be capable of checking each measured data value for consistency with other variables. Consistency checking of instrument results is a key supervisory task performed by the plant operators and it is plausible that much data supervision could be performed by computer controlled instruments. The instrument should have memory of past measurement results so it can compare the current measurement with recent values of the same measurement or some average of the recent values. The smart instrument can check the current signal trend with the trend exhibited by other variables. The smart level instrument

could be programmed to regard a deviation of the current steam generator level datum from the average of prior readings in excess of some threshold as normal if steam generator pressure is changing at some rate and abnormal if it is not. Incorporating a process model into the level instrument gives it the ability to determine if a particular measurement result is consistent with other plant variables. Since a smart instrument is envisioned as an aid to the operator, it should not require additional alarms or require significant retraining to use (reference S1). The results of the consistency checks it performs could be presented to the operator by means of a small warning message on the instrument meter face or cathode ray tube display as well as being fed to a plant data logging computer.

3.2.2 Redundancy

Redundancy must be designed into any instrument that monitors an important reactor plant variable (reference M2). It would be a serious shortcoming for an instrument providing display of and control system inputs based on a plant variable measured by a single sensor since it could lead to undesirable operator or control system response either during normal operations (e.g. failure to act on a malfunction because it is not indicated by the instrument) or in casualty situations (e.g. masking the casualty or giving inconsistent output).

The smart level instrument should have at least 2 independent level sensing signals as inputs. It is already a common procedure in power plant design to have 4 independent electric level sensing channels per steam generator so this is not an overly restrictive requirement. The smart level instrument would record and compare the two level signals at each sampling interval. Level data points

could then be averaged over a suitable number (selected to establish a desired confidence interval) of sampling intervals. In addition, the smart instrument could be programmed with an allowable deviation from the average of prior signals, either from prior knowledge or using information recorded in real time, so that sensor data points that deviated in excess of the allowable amount from would not be included in the average. If a certain number of consecutive signal samples are rejected or some threshold of total signal samples over a certain time interval is exceeded, the operator could be alerted so the affected instrument channel could be checked.

3.2.3 Filtering

The instrument designer must anticipate that the sampled data presented to the smart instrument will be subject to noise degradation. The noise would result from interference from other electrical signals, process noise, and quantization noise.

Radiation shielding considerations for the reactor and reactor building dictate that there be a minimum of penetrations in the secondary reactor shield to enhance shield structural integrity and reduce the possibility of radiation streaming. Minimizing the number of shield penetrations necessitates routing multiple electrical signal cables in bundles through a limited number of shield penetrations. If the smart instrument is located outside the secondary shield, it is a virtual certainty that cables connecting the smart instrument to its transducers will be placed in proximity to higher voltage and or frequency signal cables for other systems so that there will be crosstalk from these other signals that will reach the smart instrument input. There will probably also be a significant

noise component at 60 Hertz due to power line interference.

Process noise is composed of random signal variations introduced at the transducer input. The random component of the signal is produced by minor local variations in the measured values and the statistical nature of the physical interactions between the measured variables and the transducer. In addition, the smart instrument can be programmed to evaluate sensor performance by interpreting the character of the process noise. The instrument could either be pre-programmed with maximum and minimum tolerable values for noise variations or could determine these limits through a weighted average of prior data. This expected noise deviation data could be used to alert the operator to an abnormal sensor noise signature and thus detect otherwise undetectable sensor failures.

Quantization noise results from the inability of a digital computer to accept data in the continuous, analog form produced by the transducer. Before the smart instrument can process the sampled signal, it must first be converted to a digital representation. The resolution or accuracy of the analog to digital conversion is related to the number of binary digits, bits, used to represent the digital data. While quantization noise can be reduced by using an analog to digital (A/D) converter with more bits (at the cost of storing and transmitting more data), it is an important consideration for the designer, especially since the digital signal values will be used in various computations of model parameters.

To compensate for process noise and interference noise degradation of the sampled data, the smart instrument could be programmed to filter the incoming data digitally prior to processing in the model. It could also accept and record

the raw, unfiltered, digital data so it could be compared with the filtered data if necessary for conducting performance diagnostics. One could select a filter to remove a range of frequencies or reject a specific frequency where the majority of the noise power might be concentrated. A moving average filter would be useful for getting a good estimate of the mean signal value in the presence of noise.

One other benefit of using a digital filter is that the filter characteristics could be easily changed without requiring a redesign of the instrument or the filter could be adaptive, possibly using a matched filter, to adjust the filter parameters in real time as the information is being received.

3.3 Capabilities and Limitations

A smart instrument's capabilities include:

·**Enhanced Reliability**: a smart instrument can provide more reliable information than conventional sensors because it can include some extra variables in its model that enable it to provide reliable indication over a broader range of situations, needs fewer assumptions, and can correct transducer drift if the designer has the ability to model it.

·**Calibration Reduction**: smart instruments provide a real time means for objectively assessing the quality and accuracy of data presented, thus replacing strictly calendar based calibration requirements.

·**Variable Inference**: in some situations, a smart instrument can infer plant variables that are not directly measurable, but are desired for increasing model accuracy,

assessing instrument reliability, or for providing extra operational information.

·**Self Diagnosis**: a smart instrument can be programmed with built in test (BIT) routines to perform diagnostics on its major components and alert the operator to specific failures, thus reducing repair time.

·**Sensor Communication**: smart sensors can query other sensors for information on a common communication bus without requiring dedicated instrument to instrument connections. A control circuit could periodically poll sensors for data. Sensors could record the time when a certain reading or alarm occurs to be used for fault isolation. For example, pressurized water power plants usually have salinity cells at various locations in the condensate stream of the secondary system to detect the introduction of impurities into the condensate. Unfortunately, a large sea water leak upstream of several salinity cells will usually cause all the downstream cells to alarm nearly simultaneously so it is difficult to specify rapidly the source of the contamination, thus requiring more time to find and correct the source of the casualty. If the salinity sensors recorded the times when their alarms occurred, the operators might be able to identify more easily the source of the contamination based on the recorded alarm times. In addition, a communications channel between instruments could enable a control unit or protection circuit to query the instruments that provide it with input data, either to perform continuity checks or brief on-line diagnostics. Depending on the sampling interval and the hardware used, there could be sufficient time between data samples to do these checks.

The limitations of smart instruments include:

·**Model**: the performance benefits discussed above are limited by the quality and accuracy of the model used by the smart instrument. The model must be chosen carefully so that it is robust and not subject to oscillatory or unstable behavior.

·**Model Complexity**: the designer does not have unlimited flexibility when selecting model complexity and variables to include. The more complicated the model, the faster the central processing unit needed and the more memory that will be required. In addition, robustness tends to be a more serious issue for more complicated models.

·**Fault Tolerance**: the smart instrument must be capable of withstanding power failures and a potentially harsh operating environment. Its data presentation algorithm and model implementation must be capable of recovering from unexpectedly large and small inputs without suffering failure. The designer might decide to use some kind of battery backup for the instrument, especially if it does some of its processing based on real time variable history.

·**Interface**: computers and computer controlled devices generally exhibit the tendency to produce and display data that has the appearance of truth even when receiving faulty inputs. It is important that the data be presented to the user in a form that enables him to make a determination of the quality of the data.

Conclusions

Because it is controlled by a machine that is capable of making complicated decisions based on input data and has the ability to adapt its performance to the measured data during

operation, the smart instrument is capable of considerably more sophisticated data analysis and manipulation than a conventional instrument.

Chapter 4

Dynamics of a Steam Generator Level Sensor

The model is developed in this research to relate the pressure in the condensing pot to that in the steam generator. The model permits calculation of the superficial vapor and liquid velocities and the liquid height in the drain pipe for the two phase flow from the condensing pot to the steam generator. None of these quantities is normally measured, but a level instrument that could accurately estimate their value dynamically could alert the operator to the onset of conditions that could lead to inaccurate level information.

4.1 System Description

The purpose of the condensing pot is to ensure the reference leg of the level instrument is always filled to a constant level. During normal operation, steam flows from the generator steam space to the condensing pot via a piping connection, called the drain line or tube in this paper. In the condensing pot, the steam condenses because the condensing pot is not insulated (as noted in earlier descriptions). Some of the condensed liquid keeps the reference leg full, but the remainder spills over from the condensing pot and into the drain pipe, returning to the steam generator. The condensing pot is modeled as cylinder with its axis horizontal having the drain pipe connected to one of the circular bases.

A design aim for the drain pipe is that it be large enough to accommodate the counter-current vapor-liquid flow and remain smooth-stratified or wavy-stratified under most normal conditions. However, some combinations of drain pipe diameters and phase flow rates in the drain pipe can lead to a flow transition from wavy-stratified to either *intermittent*, in which waves at the surface are picked up to form a frothy slug which is propagated along the channel, or *annular-dispersed*, the formation of a vapor core with a liquid film around the periphery of the pipe.

Rearranging equation (1) produces:

$$P_A - P_B = (p_c - p_{sg}) + (\rho_r - \rho_v) gH - (\rho_{dc} - \rho_v) gL \quad (3)$$

As noted earlier, erroneous level indication could result from failure of the reference leg height to remain constant. As shown in figure 5, if the height of liquid in the reference leg rises above the design level (which would most likely a result of flooding in the drain pipe), the differential pressure transmitter would sense a decreased differential pressure since the effective H is actually lower. Since H is assumed by the instrument designer to remain constant under all circumstances, the instrument would interpret this change as a decrease in level. The effect of this condition on the instrument would be the presentation to the operator and to the level control system of an indicated level inconsistent with the actual level.

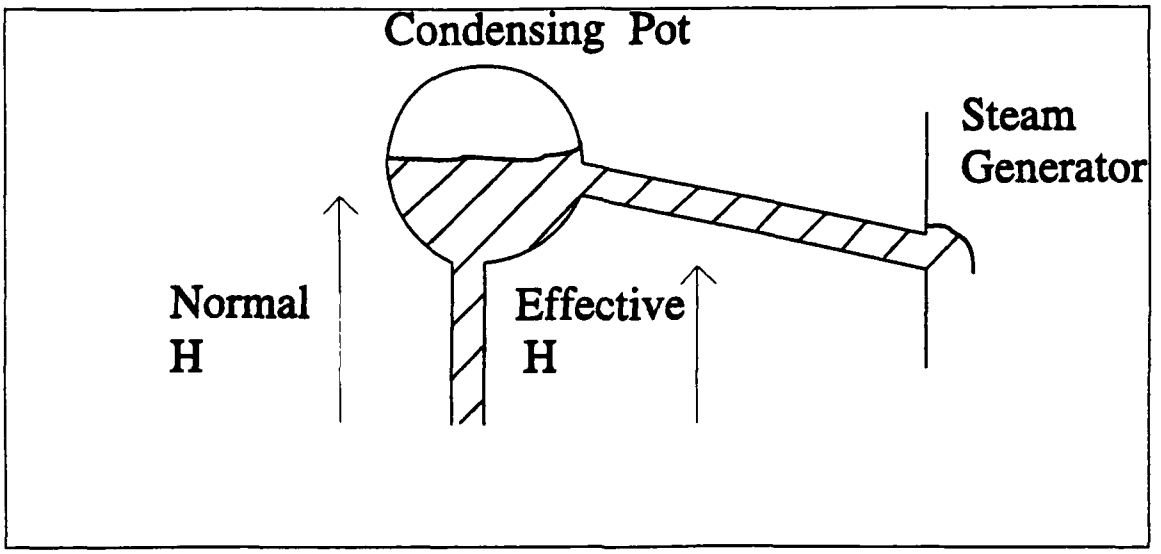

Figure 5: Effective Reference Leg Height of Flooded Condensing Pot

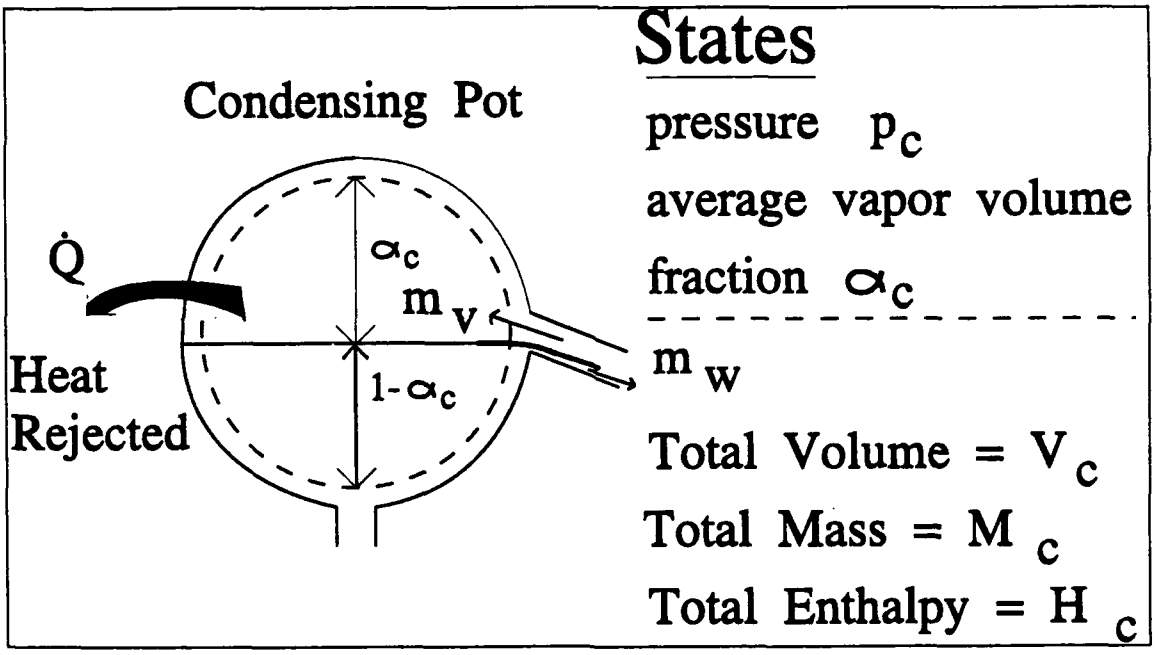

Figure 6: Condensing Pot Control Volume

For the system under consideration, the steam generator, condensing pot, and the drain pipe, two control volumes are identified. The first consists of the condensing pot. The

second is the drain pipe itself (between the condensing pot and up to the steam generator tap connection). They are depicted schematically in figures 6 and 7.

The assumptions of the following calculations are:

1. Each control volume is assumed to consist of saturated liquid and vapor in thermodynamic equilibrium under all operating conditions.
2. The drain piping, usually consisting of various sections of horizontal and vertical piping runs, is simplified to be just one section of piping, inclined from the horizontal by an angle θ. This can vary from installation to installation.
3. No significant concentration of non-condensible gases is present in the steam generator.

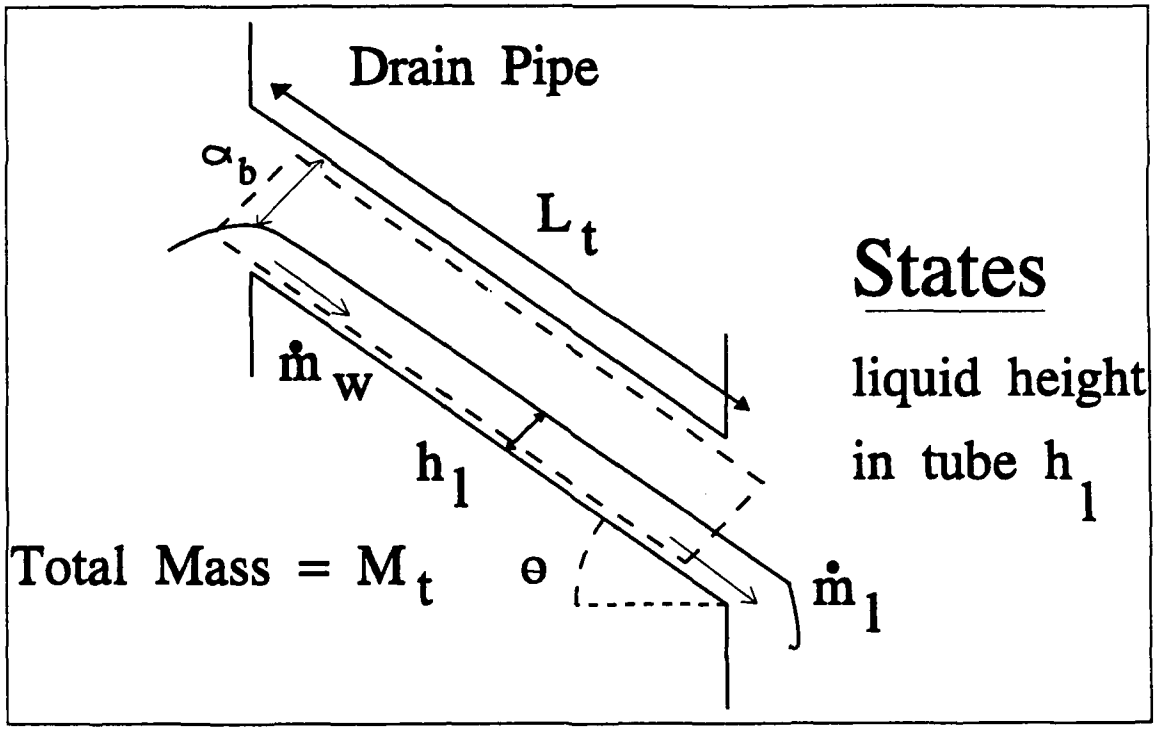

Figure 7: Drain Line Control Volume

The model inputs are: p_{sg} (pressure in the steam generator

at the tap adjacent to the drain pipe connection), p_c (pressure in the condensing pot), α_c (the average vapor fraction in the condensing pot), and h_l (the liquid height in the drain pipe). The model requires the initial values for p_{sg}, p_c, α_c, and h_l. The inclination of the drain pipe from the horizontal, θ, is assumed known.

The key difficulty when trying to incorporate features of the drain pipe flow into the overall model is how to treat and calculate the transient liquid height in the tube when steam generator pressure changes. For the purposes of this model, the connection between the two is horizontal or nearly so and the liquid surface in the condensing pot is approximately a free surface. It therefore seems reasonable to conclude that the characteristics of the flow at the transition between the condensing pot and the drain pipe are best described by open channel flow theory. The liquid flow input is varied during transients in the sense that the liquid height in the pipe at the junction with the condensing pot is the result of weir flow. The liquid mass balance in the condensing pot is a result of weir flow and the instantaneous rate of condensation in the condensing pot. The liquid height in the drain pipe closer to the steam generator is a function of the liquid and vapor velocities and the pressure gradient along the pipe.

4.2 Conservation Equations

A first equation is obtained that defines conservation of mass in the condensing pot control volume.

$$\frac{dM_c}{dt} = \rho_v j_v A - \dot{m}_w \qquad (4)$$

where M_c ▲ mass of water in the condensing pot;
ρ_v ▲ density of water vapor in the condensing pot;
j_v ▲ superficial vapor velocity of the vapor entering the condensing pot from the steam generator;
A ▲ the cross sectional area of the drain pipe; and
$\dot{m}_w$ ▲ the mass flow rate of liquid leaving the condensing pot in the weir.

Note that the superficial liquid velocity in the weir is not necessarily the same as j_l, the superficial liquid velocity in the drain pipe close to the steam generator, at least during transient conditions when the pressure of the steam generator and the condensing pot are changing with time.

Conservation of energy, in terms of enthalpy, in the condensing pot control volume gives:

$$\frac{dH_c}{dt} - V_c \frac{dp_c}{dt} = \rho_v j_v A H_v - \dot{m}_w H_l - \dot{Q} \qquad (5)$$

where H_c ▲ the total mass-enthalpy product in the condensing pot;
V_c ▲ the total volume in the condensing pot;
A ▲ the total cross sectional area of the drain pipe;
H_v ▲ the enthalpy of the vapor entering the condensing pot from the steam generator;
H_l ▲ the enthalpy of the liquid leaving the condensing pot; and
$\dot{Q}$ ▲ the heat loss from the condensing pot to ambient.

The total mass and enthalpy in the condensing pot are:

$$M_c = [\rho_l (1-\alpha_c) + \rho_v \alpha_c] V_c \qquad (6)$$

$$H_c = [\rho_l H_l (1-\alpha_c) + \rho_v H_v \alpha_c] V_c \qquad (7)$$

where ρ_l ▲ density of the liquid leaving the condensing pot.

In the drain line control volume, conservation of mass gives:

$$\frac{dM_t}{dt} = \dot{m}_w + \rho_l j_l A \qquad (8)$$

where M_t ▲ total mass of water in the drain line or tube and the influence of the vapor phase in the pipe has on the change in mass in the pipe has been neglected.

As noted earlier, it is assumed that the transient flow condition at the entrance to the drain line, at the interface to between the condensing pot and the drain line, can best be modeled as a weir. From open channel flow theory, reference C1 and L1, for steep channels, the flow is critical at the channel inlet, thus the flow energy is minimized there, yielding the critical flow condition:

$$\frac{j_{lw}}{(1-\alpha_b)\sqrt{\frac{gD_t\cos\theta}{a_l}}} = 1 \qquad (9)$$

so that:

$$\dot{m}_w = \rho_l j_{lw} A = \rho_l (1-\alpha_b) A \sqrt{\frac{gD_t\cos\theta}{a_l}} \qquad (10)$$

where j_{lw} ▲ superficial liquid velocity at the weir,
α_b ▲ vapor fraction at the boundary between the condensing pot and the top of the drain pipe,
▲ angle of elevation of drain pipe from horizontal,
g ▲ acceleration of gravity,

D_t ▲ diameter of the drain pipe, and
a_ℓ ▲ energy or coriolis coefficient.

α_b only applies in the vicinity of the weir and is not the same as the void fraction in the pipe, α_t, closer to the steam generator. The energy coefficient, a_ℓ, varies with the liquid depth and is usually determined empirically, is set equal to 2 for simplicity since, according to reference C1, experimental values of a_ℓ are in the range of 1.03 to 1.36 for fairly straight, prismatic channels. Since the precise degree to which the connection between the drain pipe and the condensing pot approximates an open channel is not known, the value for a_ℓ is taken to be 2 as a worst case estimate.

Differentiating (3) and (4)

$$\frac{dM_c}{dt} = \left(\frac{\partial M_c}{\partial p_c}\right)_{\alpha_c} \frac{dp_c}{dt} + \left(\frac{\partial M_c}{\partial \alpha_c}\right)_{p_c} \frac{d\alpha_c}{dt}$$

$$\frac{dM_c}{dt} = \left(\frac{\partial \rho_\ell}{\partial p_c}(1-\alpha_c) + \frac{\partial \rho_v}{\partial p_c}\alpha_c\right) V_c \frac{dp_c}{dt} + (\rho_v - \rho_\ell)\, V_c \frac{d\alpha_c}{dt} \qquad (11)$$

and

$$\frac{dH_c}{dt} = \left(\frac{\partial H_c}{\partial p_c}\right)_{\alpha_c} \frac{dp_c}{dt} + \left(\frac{\partial H_c}{\partial \alpha_c}\right)_{p_c} \frac{d\alpha_c}{dt}$$

$$\frac{dH_c}{dt} = \left[\frac{\partial(\rho_\ell H_\ell)}{\partial p_c}(1-\alpha_c) + \frac{\partial(\rho_v H_v)}{\partial p_c}\alpha_c\right] V_c \frac{dp_c}{dt} + (\rho_v H_v - \rho_\ell H_\ell)\, V_c \frac{d\alpha_c}{dt} \qquad (12)$$

substituting (11) and (12) into (4) and (5)

$$\left(\frac{\partial \rho_\ell}{\partial p_c}(1-\alpha_c)+\frac{\partial \rho_v}{\partial p_c}\alpha_c\right)V_c\frac{dp_c}{dt}+(\rho_v-\rho_\ell)\,V_c\frac{d\alpha_c}{dt}=\rho_v j_v A-\dot{m}_w \quad (13)$$

$$\left[\frac{\partial(\rho_\ell H_\ell)}{\partial p_c}(1-\alpha_c)+\frac{\partial(\rho_v H_v)}{\partial p_c}\alpha_c-1\right]V_c\frac{dp_c}{dt}$$

$$+(\rho_v H_v-\rho_\ell H_\ell)\,V_c\frac{d\alpha_c}{dt}=\rho_v j_v A H_v-\dot{m}_w H_\ell-\dot{Q} \quad (14)$$

The total mass in the drain line, M_t, is:

$$M_t=A_\ell L_t \rho_\ell \quad (15)$$

where L_t ≙ the total length of the drain pipe; and $A_\ell=(1-\alpha_t)A$.

Relate M_t, the total mass of water in the drain line, to h_ℓ, the liquid height in the drain line, through the following geometric relationships (see figure 8):

$$\phi_t=\cos^{-1}\left(1-2\frac{h_\ell}{D_t}\right) \quad (16)$$

$$A_{\ell t}=\left(\frac{D_t}{2}\right)^2(\phi_t-\cos\phi_t\sin\phi_t) \quad (17)$$

Substituting (16) into (15):

$$M_t=\left(\frac{D_t}{2}\right)^2(\phi_t-\cos\phi_t\sin\phi_t)\,L_t\rho_\ell \quad (18)$$

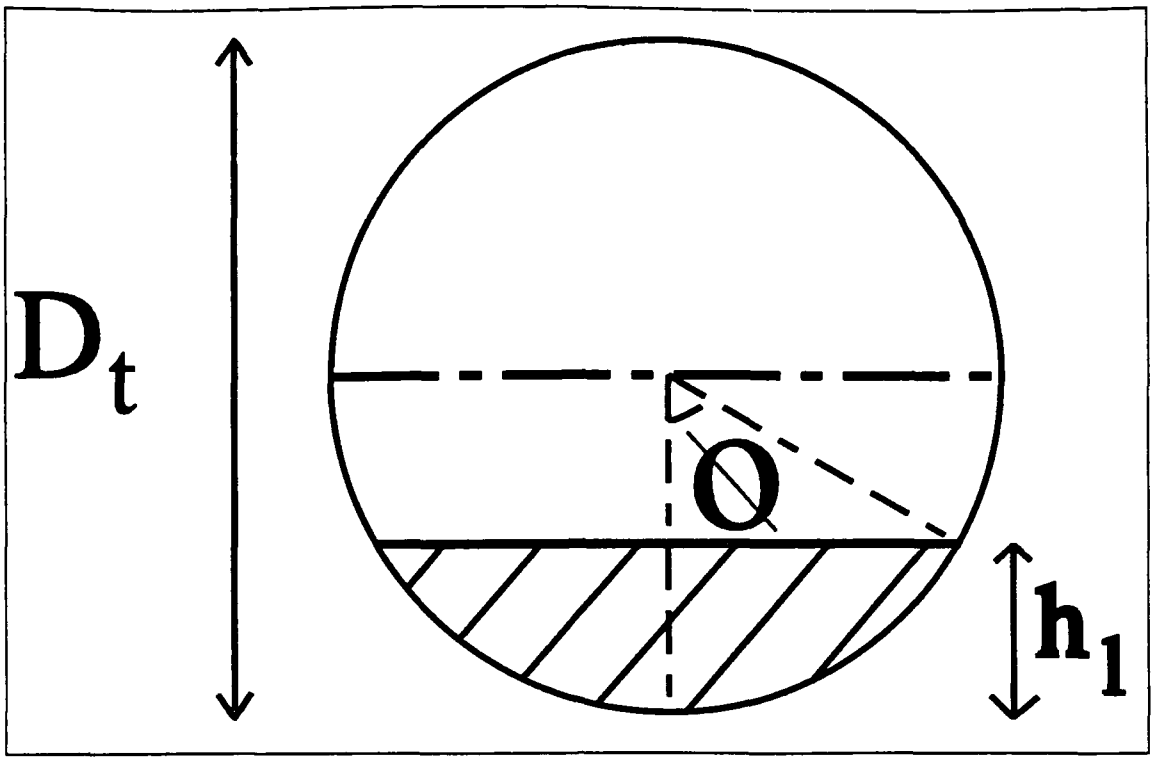

Figure 8: Relation Between h_l and ϕ in the Drain Pipe

differentiating (14)

$$\frac{dM_t}{dt} = \left(\frac{D_t}{2}\right)^2 L_t \rho_l \left(\frac{d\phi_t}{dt} - cos^2\phi_t \frac{d\phi_t}{dt} \right.$$

$$\left. + sin^2\phi_t \frac{d\phi_t}{dt} + 2sin^2\phi_t \frac{d\phi_t}{x} - 2sin^2\phi_t \frac{d\phi_t}{dt} \right) \quad (19)$$

$$\frac{dM_t}{dt} = \left(\frac{D_t}{2}\right)^2 L_t \rho_l \left(\frac{d\phi_t}{dt} - \frac{d\phi_t}{dt} + 2sin^2\phi_t \frac{d\phi_t}{dt} \right)$$

$$\frac{dM_t}{dt} = \left(\frac{D_t}{2}\right)^2 L_t \rho_l \left(2sin^2\phi_t \frac{d\phi_t}{dt} \right) \quad (20)$$

recall

$$\frac{d}{dx}(\cos^{-1}x) = -\frac{1}{\sqrt{1-x^2}}$$

Using the above formula to differentiate (16) produces:

$$\frac{d\phi_t}{dt} = \frac{2}{D_t\sqrt{4\frac{h_l}{D_t}\left(1-\frac{h_l}{D_t}\right)}}\frac{dh_l}{dt} \qquad (21)$$

substituting (21) into (20)

$$\frac{dM_t}{dt} = \frac{D_t}{2}L_t\rho_l\frac{sin^2\left[\cos^{-1}\left(1-2\frac{h_l}{D_t}\right)\right]}{\sqrt{\frac{h_l}{D_t}\left[1-\frac{h_l}{D_t}\right]}}\frac{dh_l}{dt} \qquad (22)$$

substituting (22) into (8)

$$\frac{D_t}{2}L_t\rho_l\frac{sin^2\left[\cos^{-1}\left(1-2\frac{h_l}{D_t}\right)\right]}{\sqrt{\frac{h_l}{D_t}\left[1-\frac{h_l}{D_t}\right]}}\frac{dh_l}{dt} = \dot{m}_w + \rho_l j_l A \qquad (23)$$

Combining (13), (14), and (23) into a matrix equation:

$$\underline{A}\frac{d}{dt}\vec{x} = \vec{f} \qquad (24)$$

where:

$$\underline{A} = \begin{bmatrix} A_{11} & A_{12} & 0 \\ A_{21} & A_{22} & 0 \\ 0 & 0 & A_{33} \end{bmatrix} \qquad (25)$$

and

$$\vec{x}=\begin{bmatrix} p_c \\ \alpha_c \\ h_\ell \end{bmatrix} \quad (26) \qquad \vec{f}=\begin{bmatrix} \rho_v j_v A - \dot{m}_w \\ \rho_v j_v A H_v - \dot{m}_w H_\ell - \dot{Q} \\ \dot{m}_w + \rho_\ell j_\ell A \end{bmatrix} \quad (27)$$

The entries of $\underline{\underline{A}}$ are:

$$A_{11}=\left[\frac{\partial \rho_\ell}{\partial p_c}(1-\alpha_c)+\frac{\partial \rho_v}{\partial p_c}\alpha_c\right]V_c$$

$$A_{12}=(\rho_v-\rho_\ell)\,V_c$$

$$A_{21}=\left[\left\{\frac{\partial}{\partial p_c}(\rho_\ell H_\ell)\right\}(1-\alpha_c)+\left\{\frac{\partial}{\partial p_c}(\rho_v H_v)\right\}\alpha_c-1\right]V_c$$

$$A_{22}=(\rho_v H_v-\rho_\ell H_\ell)\,V_c$$

$$A_{33}=\frac{D_t}{2}L_t\rho_\ell\frac{sin^2\left[\cos^{-1}\left(1-2\frac{h_\ell}{D_t}\right)\right]}{\sqrt{\frac{h_\ell}{D_t}\left[1-\frac{h_\ell}{D_t}\right]}}$$

4.3 The Functional Dependence of $\vec{f}$

4.3.1 j_v and j_ℓ

While equation (27) identifies the components of $\vec{f}$ used in equation (24), it is useful for computation to clearly establish the functional dependence of the individual components of the $\vec{f}$. The method for finding the

superficial velocities, j_v and j_l, is adapted from the approach used by Taitel and Dukler, reference T1. Figure 9 shows a smooth equilibrium stratified flow on which the following equations and geometric relationships are based.

A momentum balance on the liquid and vapor phases yields:

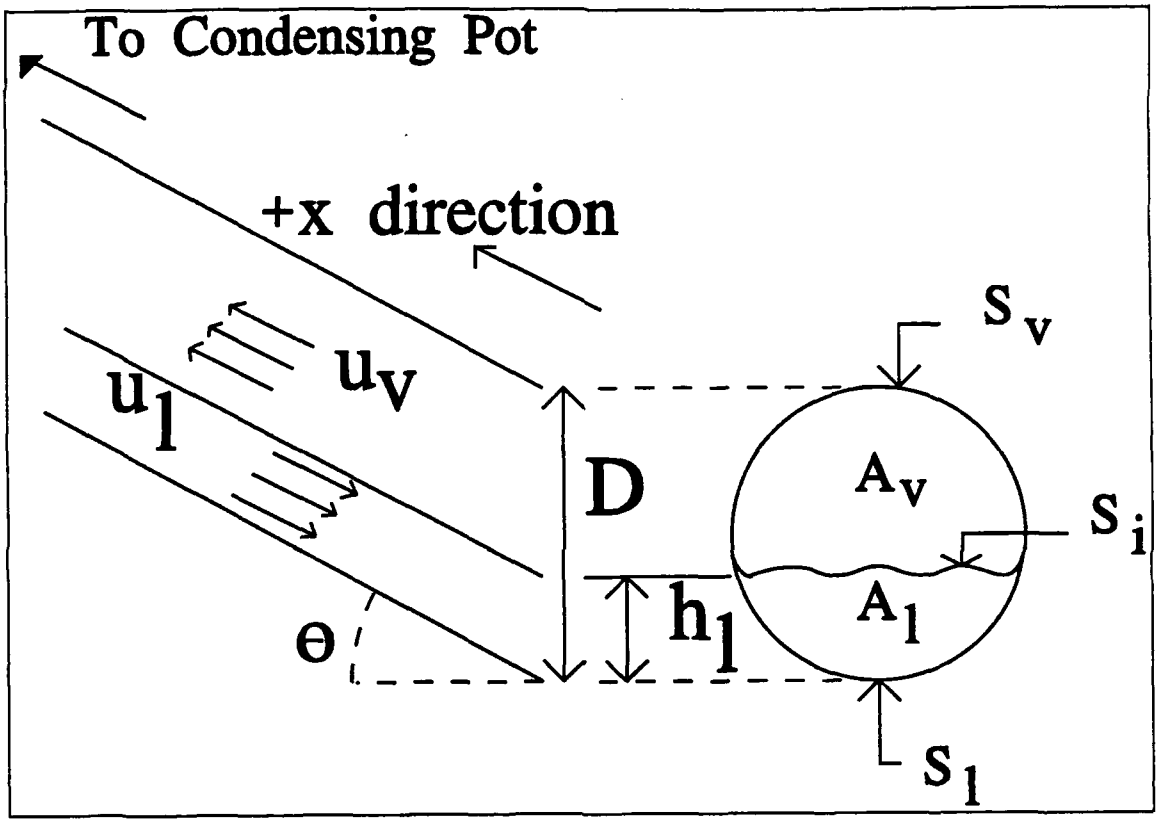

Figure 9: Two Phase Flow Geometry In Drain Pipe

$$-A_v\frac{dP}{dx}-\tau_{wv}S_v-\tau_i S_i-A_v\rho_v g\sin\theta=0 \quad (28)$$

$$-A_l\frac{dP}{dx}-\tau_{wl}S_l+\tau_i S_i-A_l\rho_l g\sin\theta=0 \quad (29)$$

where A_v ▲ cross sectional area of the vapor phase;
A_l ▲ cross sectional area of the liquid

phase;
τ_{wv} ▲ wall to vapor phase shear stress;
τ_{wl} ▲ wall to liquid phase shear stress;
τ_i ▲ interfacial shear stress;
S_v ▲ wetted perimeter of vapor phase;
S_l ▲ wetted perimeter of liquid phase;
S_i ▲ interfacial wetted perimeter; and
θ ▲ angle of pipe elevation from horizontal (see figure).

using the nomenclature from T1 and C2.

From reference T1, the geometric quantities are:

$$S_i=\phi D_t \quad where \quad \phi=\cos^{-1}\left(1-2\frac{h_l}{D_t}\right)$$

$$S_i=D_t\sin\phi$$

$$S_v=D_t(\pi-\phi)$$

$$A_v=A-A_l$$

The hydraulic diameters are:

$$D_v=\frac{4A_v}{S_v+S_i} \quad and \quad D_l=\frac{4A_l}{S_v}$$

the velocities are:

$$u_l=\frac{j_l A}{A_l} \quad and \quad u_v=\frac{j_v A}{A_v}$$

The liquid and vapor friction factors, using a Darcy Weisbach representation, are:

$$f_l=\frac{C_l}{\left[\rho_l|u_l|\frac{D_l}{\mu_l}\right]^n} \quad and \quad f_v=\frac{C_v}{\left[\rho_v|u_v|\frac{D_v}{\mu_v}\right]^n}$$

where $\mu_{v,l}$ ▲ dynamic viscosity of vapor and liquid,

respectively;

$C_{v,\ell}$ = .184; and

n = .2.

for smooth stratified flow,

$$f_i \approx f_v$$

The shear stresses are evaluated from:

$$\tau_{w\ell} = \frac{f_\ell \rho_\ell |u_\ell| u_\ell}{8} \quad , \quad \tau_{wv} = \frac{f_v \rho_v |u_v| u_v}{8}$$

$$\tau_i = \frac{f_i \rho_v |u_v - u_\ell| (u_v - u_\ell)}{8}$$

Equations (28) and (29) are 2 non-linear equations in 4 unknowns: j_v, j_ℓ, h_ℓ, and P′ (where $P' = \frac{dP}{dx}$). By defining j_v and j_ℓ as functions of h_ℓ and P′, that is:

$$j_v(P', h_\ell) \quad and \quad j_\ell(P', h_\ell)$$

equations (28) and (29) can be iteratively solved for j_v and j_ℓ in terms of h_ℓ and P′. Note that P′ is the difference between condensing pot and steam generator pressures divided by the length of the drain pipe. Equations (28) and (29) are iteratively solved for j_v and j_ℓ using known values of h and P′. Note, the equations used to solve for the superficial velocities are in error because the shear stresses above were calculated using a factor of 2 in the denominator, not 8. This error was discovered too late to re-run the simulations. The resulting sets of data were tabulated and used to correlate the superficial phase velocities given known values of liquid height in the drain pipe and pressure gradient along the pipe. The superficial velocity data is shown plotted in figures 10 and 11.

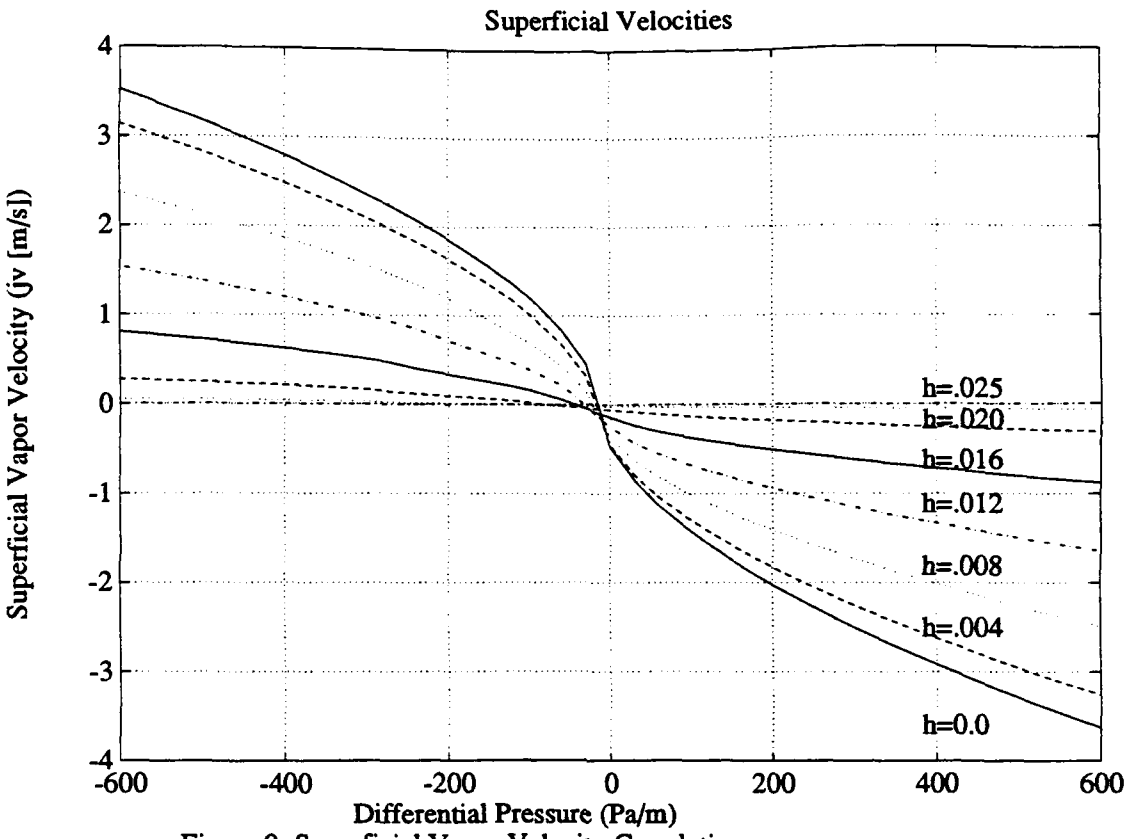

Figure 9: Superficial Vapor Velocity Correlation

Figure 10: Superficial Vapor Velocity

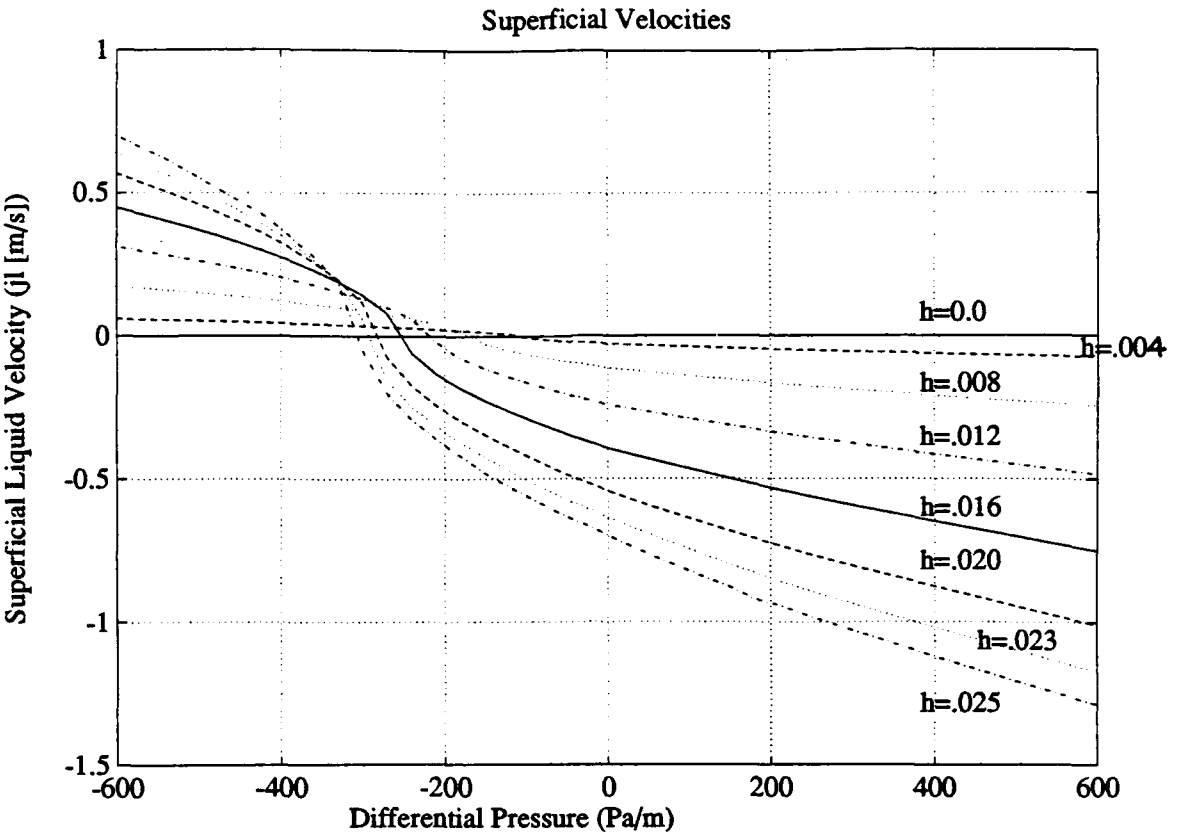

Figure 10: Superficial Liquid Velocity Correlation

Figure 11: Superficial Liquid Velocity

4.3.2 The Weir Mass Flow Rate $\dot{m}_w$

$\dot{m}_w$ is known from equation (10) using the critical flow condition, (9), but the relationship between α_b and α_c, the vapor fractions at the condensing pot-drain line interface and in the condensing pot, respectively, must be more clearly identified.

Note: α_b is the vapor fraction at the boundary between the condensing pot and the top of the drain pipe, it is not the same as the vapor fraction throughout the drain pipe.

The weir mass flow rate is:

$$\dot{m}_w = j_{lw} A \rho_l \qquad (10)$$

From the definition of α and figure 8, the following equations relate h_l to θ:

$$(1-\alpha) \triangleq \frac{A_l}{A} \qquad (31)$$

Note that these equations apply in the drain line and in the condensing pot

and

$$A_l = \left(\frac{D}{2}\right)^2 (\phi - \cos\phi \sin\phi) \qquad (17)$$

Rearranging (16)

$$\frac{2h_{lc}}{D_c} = 1 - cos\phi_c \qquad (32)$$

and solving for h_{lc} (water height in the condensing pot)

$$h_{lc} = \frac{2}{D}(1 - cos\phi_c) \qquad (33)$$

substituting (17) into (31), and letting $D=D_c$, $\phi=\phi_c$, and $\alpha=\alpha_c$ yields

$$(1-\alpha_c) = \left(\frac{D}{2}\right)^2 \left(\frac{\phi_c - sin\phi_c cos\phi_c}{A}\right) \qquad (34)$$

so that:

$$\phi_c - sin\phi_c cos\phi_c = (1-\alpha_c)\frac{A_c}{\left(\frac{D_c}{2}\right)^2} = (1-\alpha_c)\pi \qquad (35)$$

If α_c is known, (35) is used to find ϕ_c, then (33) is used to find h_{lc}. Knowing h_{lc}, h_w (liquid height at the weir, see figure 12) is found by:

$$If \quad h_{lc} < \frac{D_c - D_t}{2} \quad then \quad h_w = 0 \qquad (36)$$

$$If \quad h_{lc} > \frac{D_c + D_t}{2} \quad then \quad h_w = D_t \qquad (37)$$

$$If \quad \frac{D_c - D_t}{2} < h_{lc} < \frac{D_c + D_t}{2} \quad then \quad h_w = h_{lc} - \left(\frac{D_c - D_t}{2}\right) \qquad (38)$$

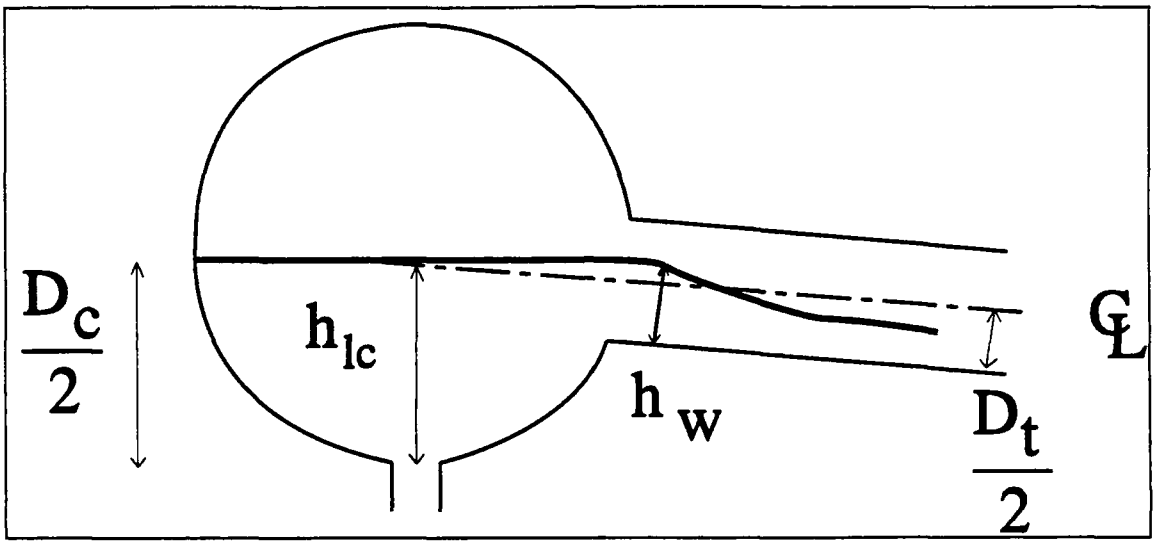

Figure 12: Relation Between h_{lc} and h_w

Where the small angular dependence of h_w is neglected. Clearly, only a certain range of h_{lc} values will produce values of h_w in the range from 0 to D_t. If h_{lc} is above the top of the drain pipe, the pipe entrance will always be filled. If h_{lc} is below the bottom of the drain pipe connection to the condensing pot, the pipe will be empty of liquid.

Once h_w is found, α_b, the vapor volume fraction at the weir, is computed from:

Now that α_b is known, $\dot{m}_w$, the liquid mass flow rate at the

$$\phi_w = \cos^{-1}\left(1 - \frac{2h_w}{D_t}\right) \quad (39)$$

$$1 - \alpha_b = \frac{A_{lw}}{A_t} = \frac{\phi_w - \sin\phi_w \cos\phi_w}{\pi} \quad (40)$$

weir present as the condensing pot-drain pipe interface, is found using equation (10):

$$\dot{m}_w = A_t \rho_l (1 - \alpha_b) \sqrt{g\left(\frac{D_t \cos\theta_t}{a_l}\right)} \quad (10)$$

4.3.3 The Heat Transfer Rate $\dot{Q}$

The heat lost from the condensing pot to the reactor building can be expressed as:

$$\dot{Q} = UA(T_{stm} - T_{air}) \quad (41)$$

UA is calculable from the geometry of the condensing pot and some empirical relations for the film heat transfer coefficients of the liquid condensing on the inner surface of the condensing pot and of the air on the outer surface.

For a cylindrically shaped condensing pot,

$$UA = \frac{1}{\frac{1}{2\pi r_{in} L_c h_{stm}} + \frac{\ln\left(\frac{r_{out}}{r_{in}}\right)}{2\pi L_c k_{st}} + \frac{1}{2\pi r_{out} L_c h_{air}}} \quad (42)$$

where
- r_{in} ▲ inner radius of the condensing pot;
- r_{out} ▲ outer radius of condensing pot;
- h_{stm} ▲ film heat transfer coefficient for the water vapor condensing on the inside surface of the condensing pot;

h_{air} ▲ film heat transfer coefficient for air in the reactor building;
k_{st} ▲ thermal conductivity of condensing pot; and
L_c ▲ inner length of condensing pot.

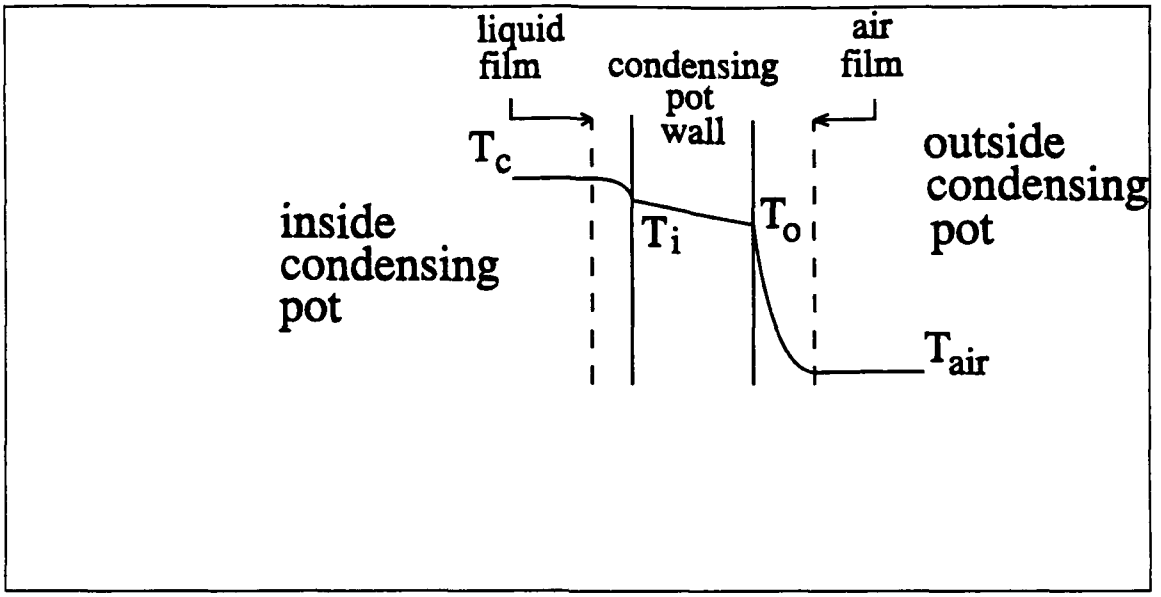

Figure 13: Condensing Pot Wall Temperature Profile

Figure 13 illustrates the typical temperature profile from the condensing pot to ambient. An empirical expression for h_{stm}, from reference M3 based on the Nusselt method for predicting the rate of heat transfer from a vapor condensing in a laminar film and running down a vertical surface, is used to get an order of magnitude estimate for the size of the film heat transfer coefficient of the condensing water vapor:

$$h_{stm} = \frac{4}{3}\frac{k}{L}Nu_l \quad where \quad Nu_l = \left(\frac{h_{fg}\rho_l^2 g L_c}{4\mu k(T_{stm} - T_{in})}\right)^{\frac{1}{4}} \qquad (43)$$

where: h_{fg} ▲ evaporation increment;
k ▲ thermal conductivity of water;
μ ▲ dynamic viscosity of water;

L_c	▲	wetted length of condensing pot above normal water level;
g	▲	acceleration of gravity;
ρ	▲	density of liquid water at condensing pot pressure;
T_{stm}	▲	Temperature corresponding to saturation pressure in condensing pot; and
T_{in}	▲	Temperature of inner surface of condensing pot;

assuming:

1. Vapor which flows parallel to the surface flows so slowly that its drag on the condensed film can be neglected.
2. Motion of any liquid element in the condensed film is governed solely by a balance of the gravity and viscous forces acting on the element, hydrostatic pressure forces and inertia forces can be neglected.

Despite the fact that the Nusselt correlation applies specifically to vertical plates, it is useful for getting an estimate of the magnitude of h_{stm}.

To estimate h_{air}, a simplified expression for the heat transfer coefficient is used, obtained from reference M1, of the form:

$$h=A\left(\frac{\Delta T}{L_s}\right)^b \quad (44)$$

where A and b are constants, depending on geometry and flow conditions, and L_s is the significant length, also depending on type of geometry and flow. Using the values suggested by reference M1 for an horizontal cylinder and laminar flow, A=.27, b=1/3, L_s is the diameter of the condensing pot, and ΔT is T_o, the outer surface temperature of the condensing pot, minus T_{amb}, the temperature of the ambient air in the reactor building. Heat transfer by radiation from the condensing pot to the reactor building, a factor that is

less than 20% of the overall heat transfer coefficient of air, is ignored. Including the contribution due to radiative heat transfer would slightly increase the value of the calculated h_{air}.

The difficulty in computing both the film heat transfer coefficients is that the value of each coefficient depends on the magnitude of the temperature difference across the respective films, which one cannot know until the heat transfer coefficient is known. The heat transfer rate from the condensing pot to the air of the reactor building, assuming that an estimate of j_t is available to compute $\dot{m}_l$, can be found from:

$$\dot{Q}=\dot{m}_l h_{fg} \quad (45)$$

where: $\dot{m}_l$ ▲ mass flow rate of liquid condensing in the condensate pot.

If the thermal resistance of the condensing steam film is known, the temperature difference across the film can be expressed by:

$$(T_{stm}-T_{in})=\frac{\dot{Q}}{R_{t_{stm}}} \text{ and } R_{t_{stm}}=\frac{1}{2\pi r_{in} h_{stm} L_c}$$

where $R_{t_{stm}}$ ▲ thermal resistance of the condensing steam film, which is a function of the temperature difference across the film.

Equation (46) can be solved iteratively to find the thermal resistance of the condensing steam film and thus h_{stm}. The same procedure is used to find h_{air}.

Figure 14 shows a typical condensing pot and drain pipe arrangement. Using a pressure of 7.34 MPa to compute h_{fg},

and an estimate of .02 for j_f, $\dot{m}_l$ and $\dot{Q}$ can be computed using equations (10) and (45), respectively. The wetted length, L_c, in equation (43) is taken as one half of 3.5 inches, the length of the condensing pot shown in figure 14, since the condensing pot is nominally half filled with liquid at all times.

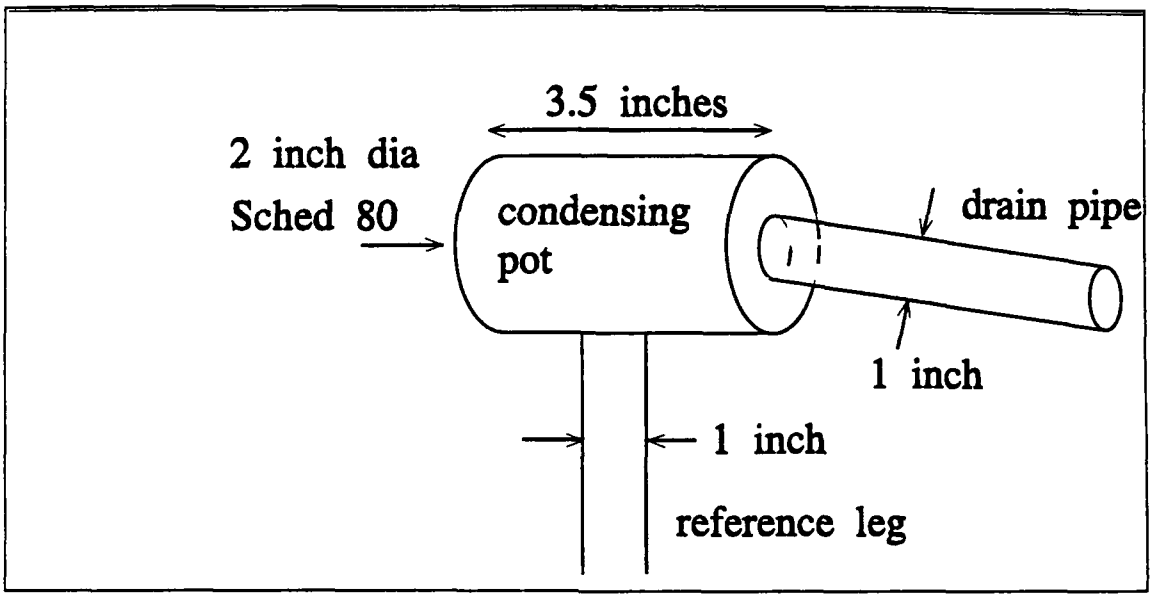

Figure 14: Geometry Of Condensing Pot

Taking k = .626 W/(m-K), g = 9.807 m/sec^2, L_c = 44.5 mm, r_{in} = 24.6 mm, μ = 90 μPa-s, ρ_l = 729 kg/m^3, an iterative solution of equation (46) and using equation (43) for h_{stm} yields a value of h_{stm} = 5400 W/(m^2-K). An iterative solution of equation (46) using the expression for h_{air} of equation (44) and assuming that h_{stm} is so large in comparison with h_{air} that its effect of the total differential temperature is negligible, gives h_{air} = 12 W/(m^2-K). Returning to equation (42), using the above values and r_{out}=27.4 mm, k_{st} = 50 W/(m-K), one finds:

$$\frac{1}{2\pi r_{in} L_c h_{steam}} = 0.000663$$

$$\frac{\ln\left[\frac{r_{in}}{r_{out}}\right]}{2\pi L_c k_{st}} = 0.008$$

$$\frac{1}{2\pi r_{out} L_c h_{air}} = 10.09$$

These results clearly show that the air film heat transfer coefficient dominates in the denominator of equation (42). For the purposes of simulation, a constant value of h_{air} is used because the actual value during transients at normal operating pressure, a function of the pressure in the condensing pot, will not vary too far from the nominal value calculated above.

The resulting functional dependence of $\dot{Q}$ is

$$\dot{Q} = UA\,(T_{stm}(p_c) - T_{air}) \qquad (47)$$

Having specified the functional forms of each component of $\vec{f}$ from equation (24), it is easier to see how to compute the necessary partial derivatives that will be needed to solve (24).

4.4 Calculations

The equations to be solved are of the form:

$$\underline{A}\frac{d}{dt}\vec{x} = \vec{f}$$

and

$$\vec{f}=\begin{bmatrix} f1 \\ f2 \\ f3 \end{bmatrix}$$

where:

$$f_1=\rho_v(p_c)\,j_v(P',h_l)\,A-\dot{m}_w(\alpha_c)$$

$$f_2=\rho_v(p_c)\,j_v(P',h_l)\,H_v(p_c)\,A-\dot{m}_w(\alpha_c)\,H_l(p_c)-\dot{Q}(p_c)$$

$$f_3=\dot{m}_w(\alpha_c)+\rho_l(p_c)\,j_l(P',h_l)\,A$$

and

$$P'=\frac{(p_c-p_{sg})}{L_t}$$

Converting to a one-step, implicit difference of the linearized equations:

$$A^n\left[\frac{\vec{x}^{n+1}-\vec{x}^n}{\Delta t}\right]=\vec{f}^n+\left(\frac{\partial\vec{f}}{\partial\vec{x}}\right)^n(\vec{x}^{n+1}-\vec{x}^n)$$

and we seek $\vec{x}^{n+1}$:

$$\vec{x}^{n+1}=\left[\frac{A^n}{\Delta t}-\left(\frac{\partial\vec{f}}{\partial\vec{x}}\right)^n\right]^{-1}\vec{f}^n+\vec{x}^n \quad (48)$$

4.4.1 The Jacobian of the f vector

The Jacobian of $\vec{f}$ is computed using numerical differentiation, where the Jacobian component in row i column j is:

$$\left(\frac{\partial \vec{f}}{\partial \vec{x}}\right)_{ij} = \frac{f_i(x_j+\Delta x_j) - f_j(x_j)}{\Delta x_j}$$

Of course, it is important to choose the Δ value small enough to avoid errors due to nonlinearity of the subject functions and large enough to avoid roundoff in getting a meaningful average value for the derivative. Several plots of the functions f_1, f_2, and f_3 were computed to estimate adequate Δ values. The values used are:

$$\Delta p_c = 30 \quad \Delta \alpha_c = .0005 \quad \Delta h_l = .0005$$

The complete Jacobian, $\frac{\partial \vec{f}}{\partial \vec{x}}$ of $\vec{f}$ is:

$$\left(\frac{\partial \vec{f}}{\partial \vec{x}}\right)^n = \begin{bmatrix} \frac{\partial f_1}{\partial p_c} & \frac{\partial f_1}{\partial \alpha_c} & \frac{\partial f_1}{\partial h_l} \\ \frac{\partial f_2}{\partial p_c} & \frac{\partial f_2}{\partial \alpha_c} & \frac{\partial f_2}{\partial h_l} \\ \frac{\partial f_3}{\partial p_c} & \frac{\partial f_3}{\partial \alpha_c} & \frac{\partial f_3}{\partial h_l} \end{bmatrix}$$

For details on the software used to solve equation (41) for various initial conditions of $\vec{x}$ and pressure transients in the steam generator, please refer to the Appendix.

4.4.2 Geometry and Initial Conditions

For the purposes of these calculations, the following average parameters were used:

Length of drain piping (L_t) =2.5 m;
Reactor building ambient air film heat transfer coefficient

(h_{air})=11 W/(m^2-K);
Inner radius of condensing pot (r_{in})=24.6 mm;
Outer radius of condensing pot (r_{out}) = 27.4 mm;
Ambient temperature of Reactor Building (T_{amb})=50°C

To calculate the initial or steady state values of $\vec{x}$, a initial value for p_c is assumed. Knowing this variable and the ambient reactor building temperature, equation (46) is used to find $\dot{Q}$, the heat rejected by the condensing pot to ambient. With $\dot{Q}$ known, the liquid mass flow rate from the condensing pot the steam generator is found from equation (45).

Equation (10) is used to compute the superficial phase velocities, presuming that the liquid and vapor mass flow rates are equal at steady state. Once j_v and j_l are known, equations (28) and (29) are solved iteratively until values for h and P′ are found. With a calculated P′ and a known value of p_{sg}, p_c can be computed and the process repeated until convergence is obtained for a value of p_c. This is how the steady state values of $\vec{x}$, composed of p_c, α_c and h_l were computed. This process is diagrammed schematically below:

$$p_c \rightarrow \dot{Q} \rightarrow \dot{m}_w \rightarrow h_w \rightarrow \alpha_c$$

$$\searrow$$

$$\begin{pmatrix} j_v \\ j_l \end{pmatrix} \rightarrow \begin{pmatrix} h_l \\ P' \end{pmatrix}$$

The above procedure for computing the initial conditions based on a combination of steam generator pressure, p_{sg}, an assumed pressure gradient between the condensing pot and steam generator, P′, and the geometry of the condensing pot.

It is, however, possible to calculate a liquid mass flow rate from the condensing pot to the steam generator, $\dot{m}_w$, that makes it impossible to solve the momentum balance equations for the liquid and vapor phases in the drain pipe, equations (28) and (29). Recall that at steady state, liquid superficial velocity in the drain pipe, j_ℓ, is related to $\dot{m}_w$ strictly by the liquid density and the pipe cross sectional area (equation (10)). Reference W1 notes that a plot of j_ℓ and j_v for constant liquid height, h_ℓ, figure 23 for the tabular data calculated, enables one to identify graphically the regions of permissible operation in the drain pipe. Positive j_v and positive j_ℓ represents cocurrent flow up from the steam generator to the condensing pot using the positive sense shown in figure 7. Negative j_v and negative j_ℓ represents cocurrent down flow from the condensing pot to the steam generator. The region of positive vapor flow and negative liquid flow between the axes and the locus of points joining tangent lines to the lines of constant vapor liquid height, called the flooding line, represents the limited region of counter current flow, where solutions are possible (see figure 23). Operation above and to the left of the flooding line is not possible, because the drain pipe is already flooded at that point. If, while calculating the steady state solution, one picks assumed conditions of pressure gradient, P', that results in superficial velocities that are beyond the flooding line, one must continue to select a lower pressure gradient and recalculate the superficial velocities until physically realizable values of the superficial velocities are obtained.

4.4.3 Model Limitations

The tabular data, values of j_v and j_ℓ for known values of h_ℓ and P', must be calculated before implementing the other model equations. The limits of the allowed liquid heights in the drain pipe are determined by the drain pipe diameter, but the range of potential pressure gradients cannot be known until after the model is implemented and some solutions calculated. The possibility exists for steam generator pressure changes to occur rapidly enough for the pressure gradient between condensing pot and steam generator encountered during transients to exceed the maximum or minimum values of P' used to compute the tables of j_ℓ and j_v data. To account for this possibility, there are two options. First, perform extensive tests of the model using the worst case positive and negative steam generator pressure transients and expand the range of drain pipe pressure gradients used to generate j_v and j_ℓ by trial and error. This is fairly easily, though tediously, accomplished and only increases the memory that the smart instrument must have. Second, if the smart instrument is capable of performing the calculations rapidly enough, the designer could elect to solve equations (28) and (29) at each time step rather than relying on tabular data computed in advance.

4.4.4 Solutions

The independent variable in the implicit difference equation (45) is p_{sg}, steam generator pressure. Equation (48) is solved for the state variables condensing pot pressure, p_c, condensing pot vapor volume fraction, α_c, and drain pipe liquid level, h_ℓ, for both constant steam generator pressure and up and down steam generator pressure ramps.

4.4.4.1 Constant Pressure

Table 1 show the results of the solutions computed at a steam generator pressure of 7.34 MPa and various condensing pot and drain pipe diameters.

Steam Generator Pressure = 7.34 MPa			Pct Chg		Pct Chg
Condensing Pot Diameter (mm)	50.8	50.8	0	54.8	7.9
Drain Pipe Diameter (mm)	25.4	27.4	7.9	27.4	7.9
$(p_c - p_{sg})$ (Pa)	-183.19	-143.16	21.9	-143.16	21.9
Condensing Pot Vapor Volume Fraction α_c	.7123	.741	4.0	.724	2.3
Drain Pipe Liquid Level h_f (mm)	5.47	4.84	11.5	4.84	11.5

Table 1: Steady State Solutions for Constant Steam Generator Pressure

A nominal steam generator pressure of 7.34 MPa was chosen since many commercial steam generators operate between 7.6 MPa and 6.9 MPa when steaming at normal operating pressure. The piping dimensions are varied to see the influence of dimensional tolerances on the stability of equation (48). As the data in table 1 shows, P′ is the most sensitive state variable with respect to the diameter of the drain pipe. A 7.9 percent increase in drain pipe diameter reduced the pressure drop by 21.9 percent, the vapor volume fraction rose by only 4 percent and the liquid level decreased by only 11.5 percent. Physically, it makes sense that enlarging the drain pipe diameter would reduce the wall friction forces, thus reducing the pressure drop. The vapor volume fraction would also decrease since expanding the pipe diameter reduces the liquid level in the pipe. The last column of table 1 indicates that condensing pot vapor volume

fraction is the only state variable sensitive to condensing pot diameter and only weakly at that. One should also note that the pressure drop between the condensing pot and the steam generator is an extremely small fraction of steam generator pressure, about .0025 percent.

4.4.4.2. Pressure Ramps

Table 2 shows the steady state solutions reached for equal and opposite steam generator pressure ramps of 300 kPa, both starting from 7.34 MPa. Pressure ramps were used as a first approximation for the generator pressure changes that result from changes in turbine loading.

		Down Ramp	Up Ramp
Pressure Ramp (kPa)	0	-300	+300
$(p_c - p_{sg})$ (Pa)	-184.19	-184.46	-179.42
Condensing Pot Vapor Volume Fraction α_c	.7123	.7144	.7102
Drain Pipe Liquid Level h_f (mm)	5.47	5.44	5.51

Table 2: Steady State Solutions for Pressure Ramps

The trend of the steady state data corresponds well to what is predicted by the physical situation. For the negative pressure ramp, lower pressure in the steam generator results in less condensation in the condensing pot and reduced heat transfer from the condensing pot to ambient since the

condensing pot is assumed to be saturated and thus the temperature of the water vapor in the condensing pot is lower for the lower pressure. Reduced condensation in the condensing pot results in a lower liquid level there which causes the liquid level in the drain pipe to be lower (from equations (36) to (38)). The opposite trend is observed for the positive pressure ramp.

As mentioned in section 4.5.3, since the values of P′ used to solve equations (28) and (29) for j_v and j_ℓ were specified in advance of computing the solution to equation (48), the possibility exits that transient values of P′ outside the ±600 Pa/m range those used might result. Preventing this form occurring constrains the maximum allowable rates of steam generator pressure change that my model could accept. As shown in table 3, the maximum allowed steam generator pressure gradient with respect to time is also different for up and down pressure transients.

Generator Pressure Ramp	Maximum Rate of Change
Down	1.33 kPa/sec
Up	.42 kPa/sec

Table 3: Maximum Generator Pressure Gradients

For the negative pressure gradient, figures 15 through 18 show the transient steam generator pressure, the differential pressure between the condensing pot and steam generator, the vapor volume fraction, and liquid height in the drain pipe. Note that both the differential pressure and the drain pipe liquid height asymptotically approach constant values during the transient, but rapidly converge toward their steady state values after the transient. It is

particularly interesting to note that the these solutions to equation (41) show that the steam generator level model is capable of directly inferring the proximity to a flooding condition because an instantaneous value of liquid height is calculated during the transient. Other methods of predicting flooding rely on correlations between the superficial liquid and vapor velocities in the pipe since liquid height in the pipe is not usually calculated.

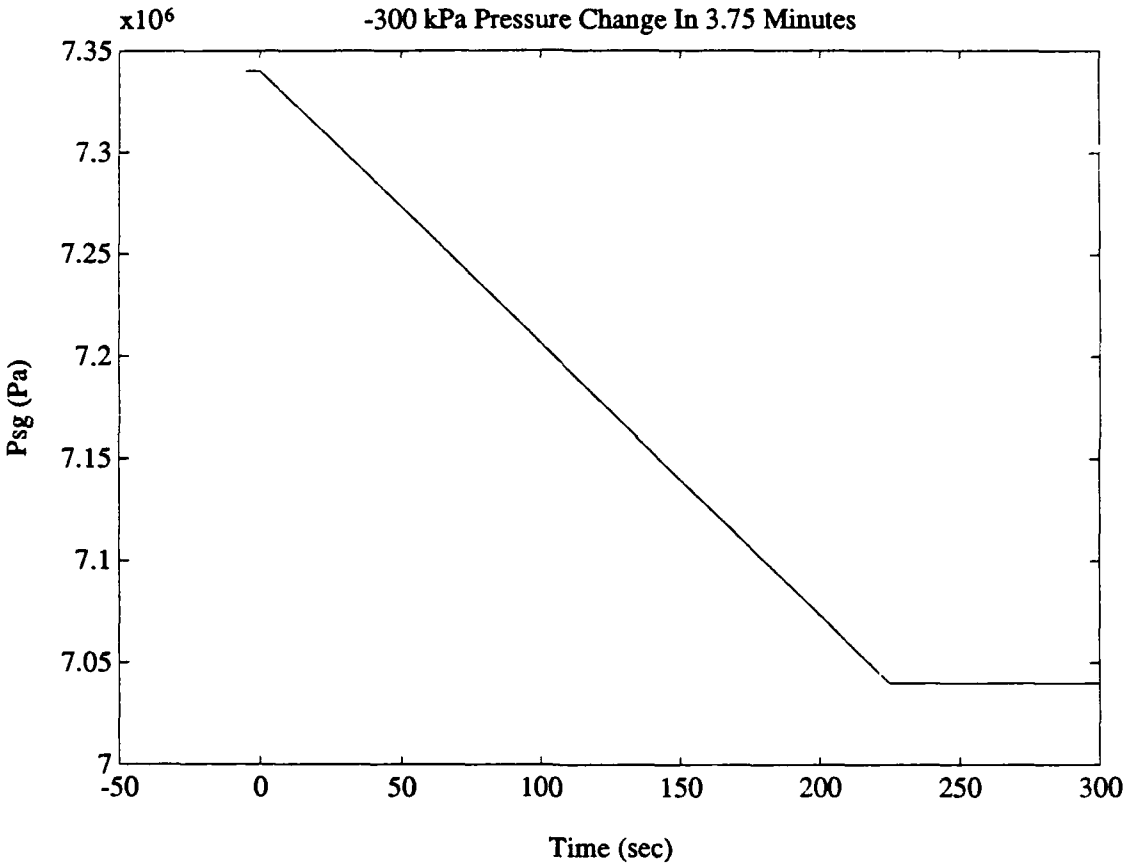

Figure 15: -300 kPa Pressure Ramp, p_{sg}

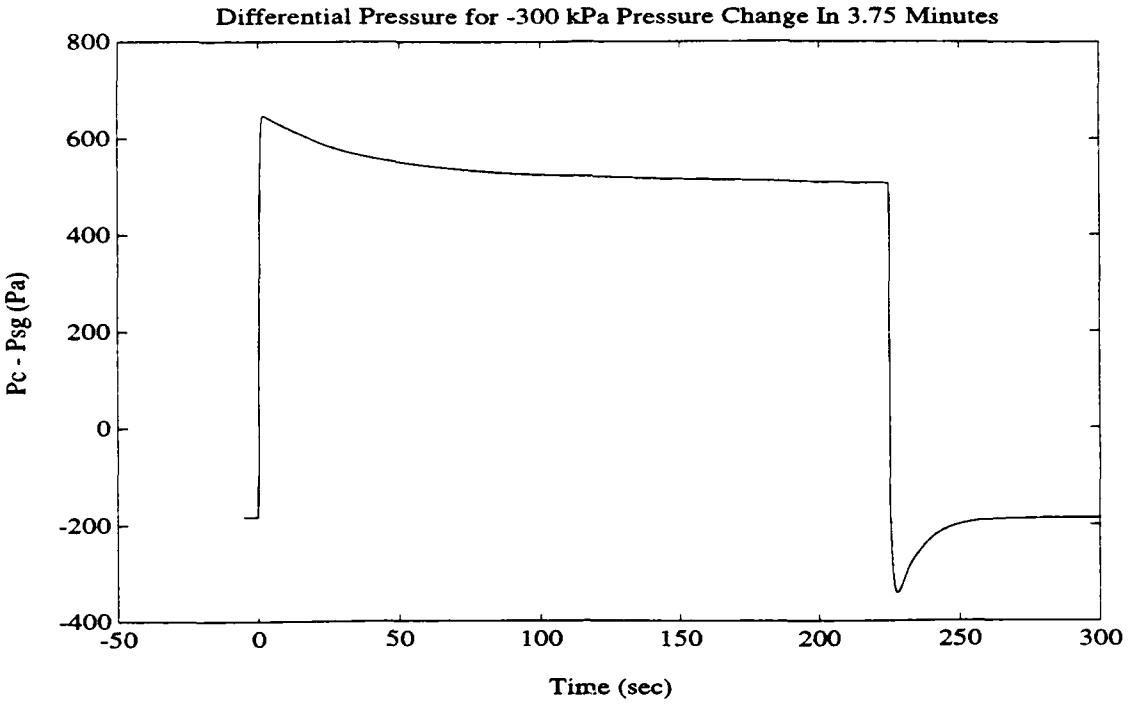

Figure 16: -300 kPa Pressure Ramp, $p_c - p_{sg}$

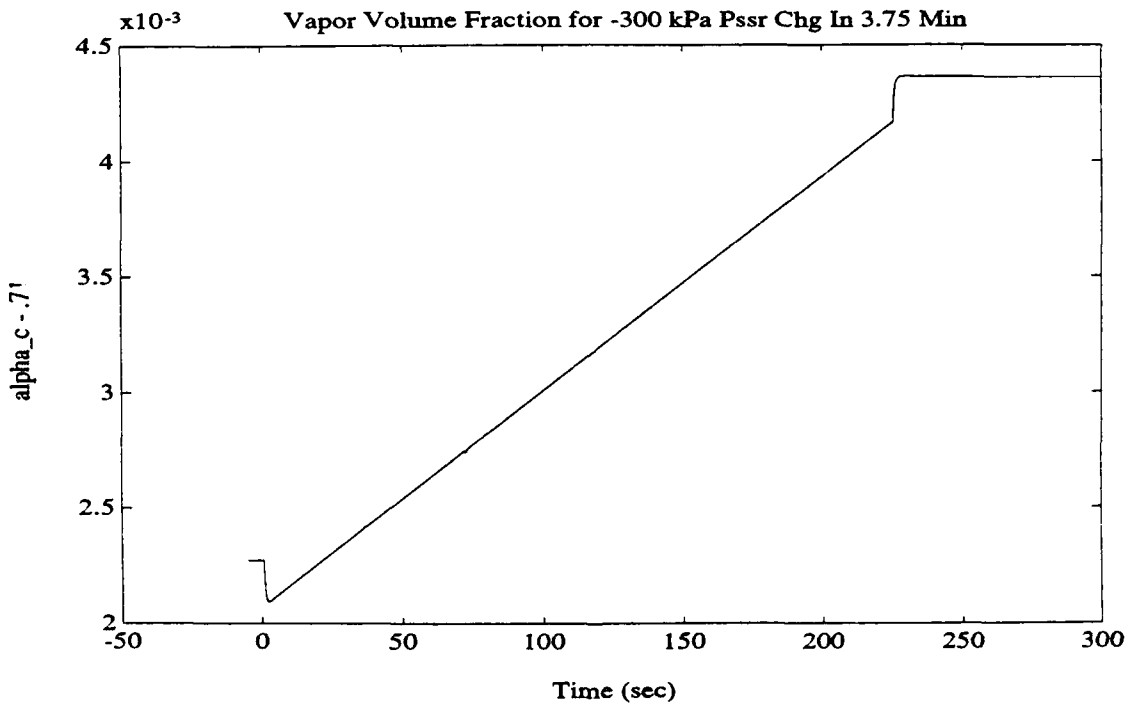

Figure 17: -300 kPa Pressure Ramp, α_c

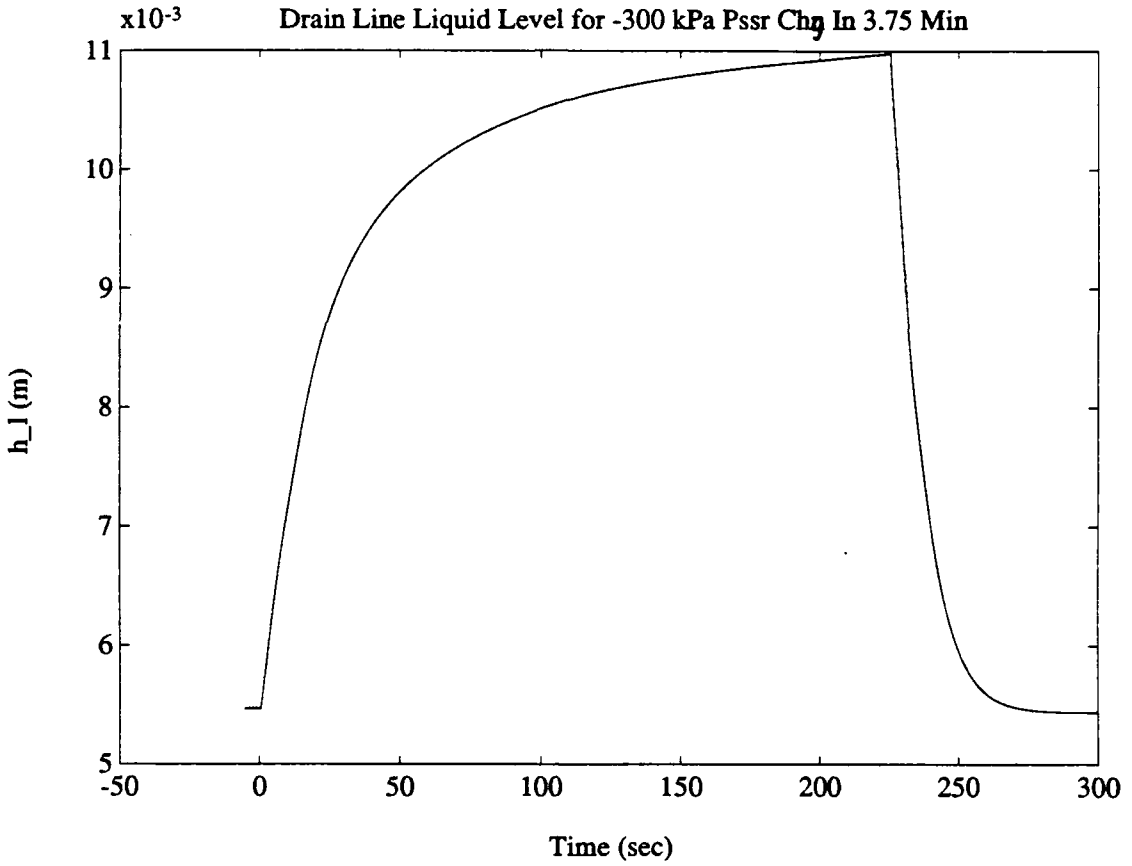

Figure 18: -300 kPa Pressure Ramp, h_t

Figures 19 through 22 show the transient steam generator pressure and state variables for the positive steam generator pressure ramp. As discussed, the positive pressure ramp had to occur over a time interval 3 times longer than that for the negative ramp in order to reach a solution. It is interesting to note that for the positive pressure transient, the transient liquid height in the tube increases just as it did for the negative pressure transient.

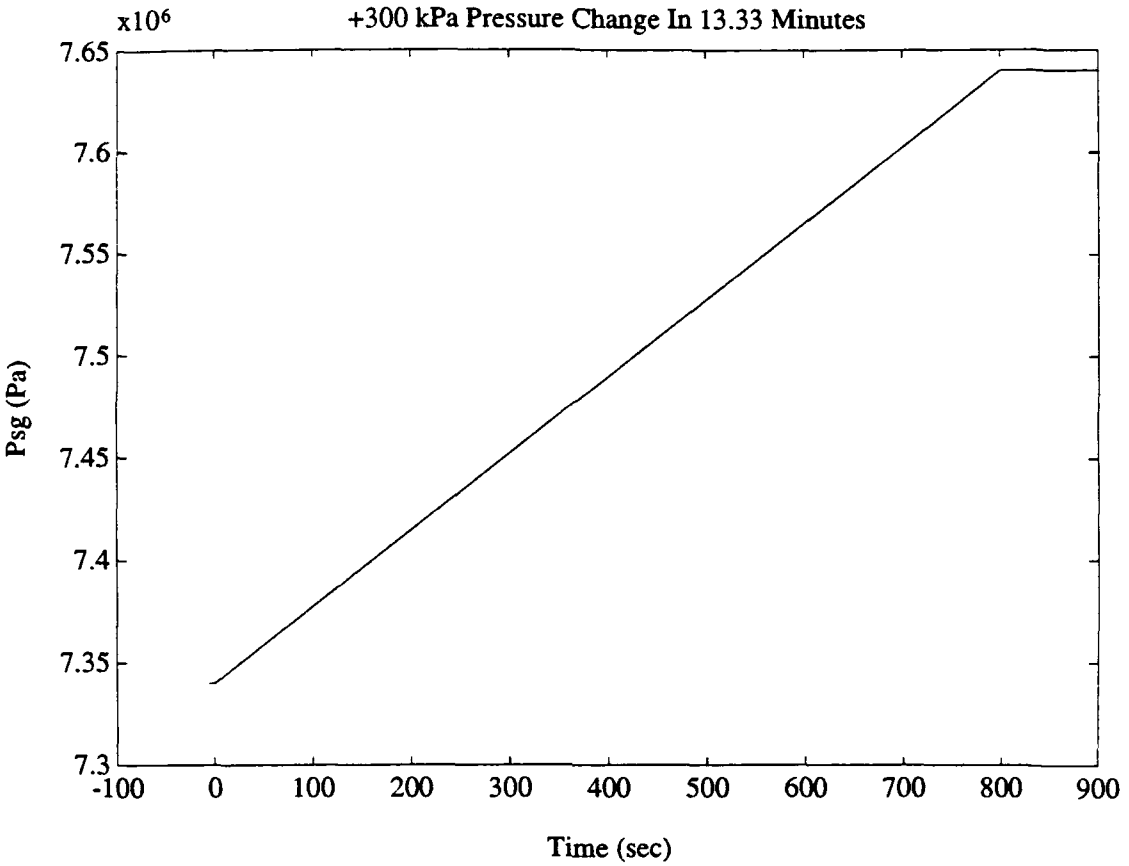

Figure 19: +300 kPa Pressure Ramp, p_{sg}

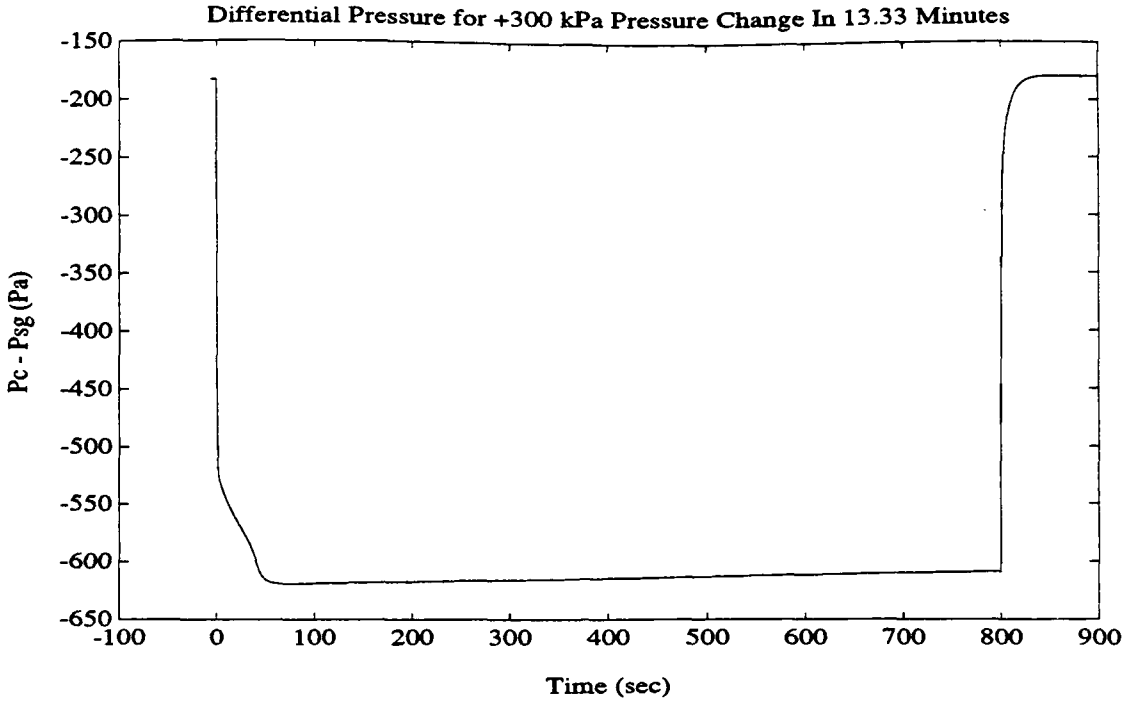

Figure 20: +300 kPa Pressure Ramp, $p_c - p_{sg}$

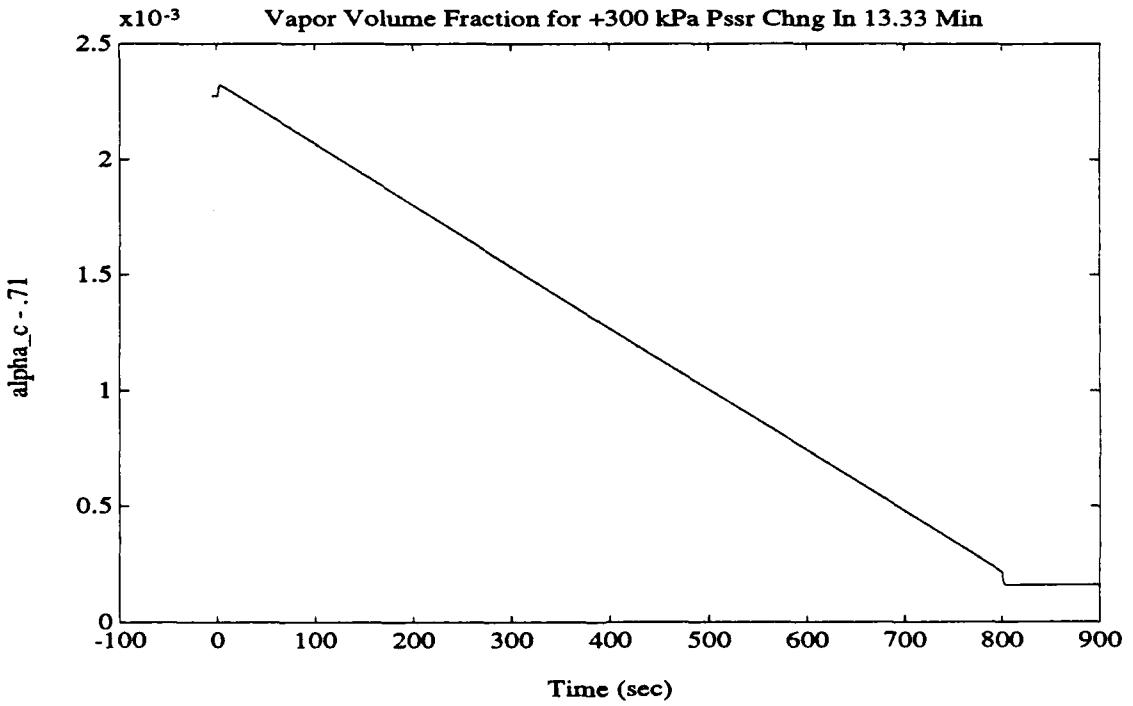

Figure 21: +300 kPa Pressure Ramp, α_c

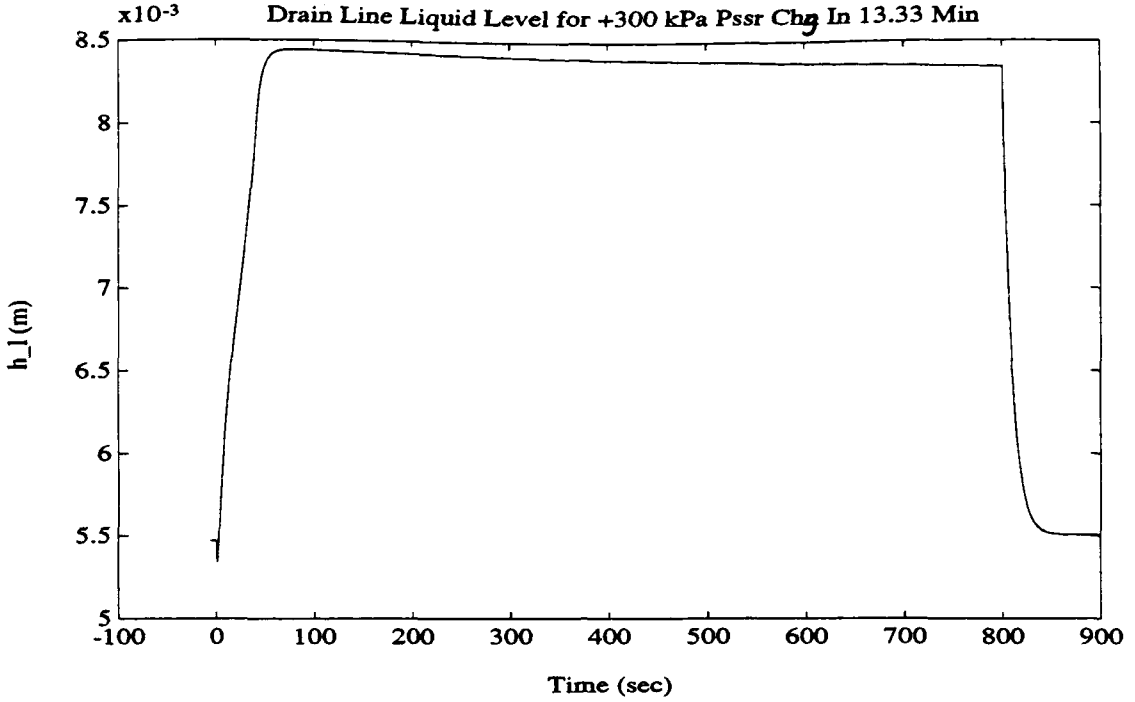

Figure 22: +300 kPa Pressure Ramp, h_f

For the negative pressure ramp, the rising trend in drain pipe liquid height can be explained as follows:

1. $(p_c - p_{sg})$ changes from negative to positive as soon as steam generator pressure begins to decrease because condensing pot pressure cannot change as rapidly as steam generator pressure.
2. To balance the momentum equations, (28) and (29), j_v must become less than zero (see figure 10, j_v must be less than zero when $p_c - p_{sg}$ becomes greater than zero).
3. Since the initial change in p_c is small, α_c remains constant or changes slowly at the start of the transient, suggesting that h_f is initially constant.
4. Looking at figure 23, if j_v becomes negative and h_f remains constant, j_l must become more negative as well,

possibly by a factor of 2 to 3.

5. Figure 11 shows that as j_l becomes more negative for a fixed value of P', h_l rises.

For the positive pressure ramp, the rising trend in drain pipe liquid height can be explained as follows:

1. $p_c - p_{sg}$ becomes even more negative as soon as steam generator pressure begins to increase.
2. To balance the momentum equations, (28) and (29), j_v must become more positive (see figure 10, j_v must increase when $p_c - p_{sg}$ becomes more negative).
3. Since the initial change in p_c is small, α_c remains constant or changes slowly at the start of the transient, suggesting that h_f is initially constant.
4. Looking at figure 23, if j_v becomes more positive and h_l remains constant, j_l must become less negative.
5. Figure 11 shows that as j_l becomes less negative for a fixed value of P', h_f rises. h_l would actually *decrease* if the P' only became slightly more negative.

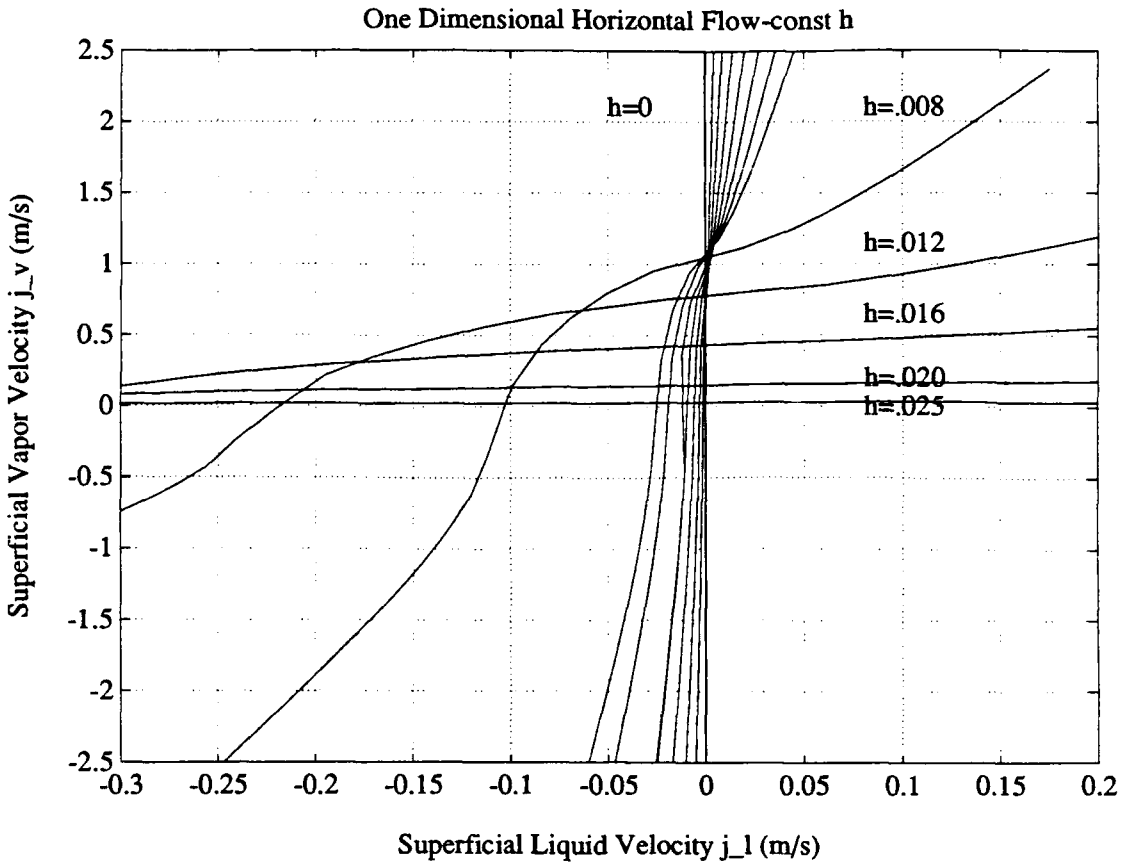

Figure 23: Flow Map for Drain Pipe

4.5 Flow Transitions

A major goal of the steam generator water level model is to create an instrument sophisticated enough to alert the operator of the approach to flooding conditions in the drain pipe. If flooding does not occur, the pressure difference across the drain pipe remains very small so no correction is required. Recall that the drain pipe returns the overflow of condensed steam from the condensing pot to the steam generator and should be sized large enough to transport the maximum expected condensation flow without undergoing a flow transition from stratified flow to annular or intermittent

flow. Such a flow transition changes the height of the reference leg and produces erroneous level readings.

4.5.1 Taitel and Dukler

Taitel and Dukler (reference T2) developed a theoretical model for predicting the onset of flow regime transitions in near-horizontal piping that agrees well with experimentally observed results.

The procedure was first to visualize a stratified liquid and then the mechanism describing the change from stratified flow. Beginning with stratified flow, as the liquid velocity increases, the liquid level rises and a wave is formed which grows rapidly, tending to block the flow. At lower vapor velocities, the wave crest forms a complete bridge and slug or plug flow results. At higher vapor velocities, there is insufficient liquid flowing to maintain or even form the bridge and the liquid in the wave is swept up around the pipe to form an annulus with some entrainment if the vapor velocity is high enough.

Taitel and Dukler found that the criterion for the transition from stratified to intermittent and to annular dispersed flow is:

$$F^2\left[\frac{1}{C_2^2}\tilde{u}_v\frac{\frac{d\tilde{A}_l}{d\tilde{h}_l}}{\tilde{A}_v}\right]\geq 1 \quad (48)$$

where F is the Froude number modified by the density ratio:

$$F=\sqrt{\frac{\rho_v}{\rho_l-\rho_v}}\frac{j_v}{\sqrt{D_t g\cos\theta}} \quad (49)$$

C2 is estimated as $1-h_l/D_t$ and the dimensionless values in

equation (48), signified by a ~, are found as follows.

$$\frac{d\tilde{A}_\ell}{d\tilde{h}_\ell}=\sqrt{1-(2\tilde{h}_\ell-1)^2}$$

$$\tilde{h}_\ell=\frac{h_\ell}{D_t}$$

$$\tilde{A}_v=\frac{1}{4}\left[\cos^{-1}(2\tilde{h}_\ell)-(2\tilde{h}_\ell-1)\sqrt{1-(2\tilde{h}_\ell-1)^2}\right]$$

$$\tilde{A}_\ell=\frac{1}{4}\left[\pi-\cos^{-1}(2\tilde{h}_\ell)-(2\tilde{h}_\ell-1)\sqrt{1-(2\tilde{h}_\ell-1)^2}\right]$$

$$\tilde{A}=\tilde{A}_v+\tilde{A}_\ell$$

$$\tilde{u}_v=\frac{\tilde{A}}{\tilde{A}_v}$$

Clearly, if one knows the liquid height in the drain pipe and the superficial vapor velocity, j_v, the proximity to the Froude number characteristic of the flow transition can be calculated from equations (48) and (49). The chief obstacle to directly implementing a scheme to evaluate the Froude number is that the superficial velocities and liquid height in the drain pipe between the condensing pot and the steam generator are not measured. Despite the numerical error that was made when computing the shear stresses in equations (28) and (29), the results of section 4.4 suggest that it is theoretically possible to infer these variables from knowledge of the steam generator pressure and piping geometry.

4.5.2 Drift Flux Model

As discussed, the flow in the drain pipe is normally two phase, counter current flow, with steam flowing from the steam space of the steam generator to the condensing pot and condensate returning from the condensing pot to the steam generator, illustrated in figure 9. The drift flux model, presented in reference W1, a separated flow model focusing on the relative motions of the individual phases in the pipe, is well suited to analysis of bubbly and slug regimes of gas-liquid flows and is appropriate to the situation at hand.

The limit of counter-current flow, called flooding as the pipe fills completely with liquid, predicted by the drift flux model can be seen on a plot of solutions of the momentum balance equations, (28) and (29), for constant liquid height in the drain pipe. Such a curve is plotted in figure 23, with superficial liquid velocities plotted horizontally and superficial vapor velocities plotted vertically, with each curve representing a different drain pipe liquid height. The region of negative liquid velocity and positive vapor velocity, called the limited region of counter current flow in reference W1, is bounded by the axes and the dotted line known as the flooding line. The flooding line is the locus of points tangent to the j_f, j_v curves in the limited counter-current flow region, since an increase in the magnitude of either phase velocity beyond the flooding line is condition for which no steady flow solution is possible and a flow transition must occur.

Conclusions

The suggested model, reflecting the influence of important physical features for processes influencing the measurement,

produces solutions that are stable and finite for both constant steam generator pressure and steam generator pressure gradients. Although a numerical error was made when solving the two phase flow equations (equations (28) and (29)), the steady state solutions appear to correspond well to the physical situation. The solutions produced for steam generator pressure ramps indicate that a potential shortcoming of the model is that some transients might cause the differential pressure between the condensing pot and the steam generator to exceed the values of differential pressure used to pre-compute superficial liquid and vapor velocities in the drain pipe.

Chapter 5

Smart Instrument Applied to Steam Generator Level

Having postulated a steam generator level measurement model capable of determining the pressure in the condensing pot and the liquid level in the drain pipe as functions of time, is appropriate to consider how successful a smart instrument including such a model might be at improving the accuracy of level measurement over a standard level sensing device. Since no operational plant level data is available for comparison, the Prism (reference K1) program is used to generate steam plant data for an up power and a down power transient at high power.

5.1 Sensor Dynamics, Information

The relationship between steam generator water level and the differential pressure cell output is:

$$L=\frac{(p_c-p_{sg})-\Delta P}{[\rho_{dc}(T_{dc})-\rho_v(p_{sg})]g}+\left(\frac{\rho_r(T_{amb})-\rho_v(p_{sg})}{\rho_{dc}(T_{dc})-\rho_v(p_{sg})}\right)H \quad (51)$$

Equation (51) is the same as equation (2), except that the functional dependence of all the variables has been specified. Thus the liquid density, ρ_{dc}, is a function of the temperature in the downcomer, the vapor density, ρ_v, is a function of the steam generator pressure, and the reference leg liquid density, ρ_r, is a function of the ambient temperature in the reactor building.

For a conventional level instrument, we can make some simplifications to make the level easier to compute. Over the pressure range usually encountered in commercial power reactors between 0 and 100 percent power, the vapor density changes from 36.5 kg/m^3 to 39.5 kg/m^3 so using an average value of 38.0 kg/m^3 for the vapor density introduces an error of no more than 4 percent. Assuming that the reactor building ambient temperature does not change, the reference leg density can be regarded as constant at 988 kg/m$_3$. The conventional instrument can also neglect the pressure differential between the generator and the condensing pot.

5.2 Downcomer Temperature Effects

As noted in the description of steam generator internals, the steam generator downcomer is the region between tube sheet wrapper and the generator vessel, below the feedwater inlet ring. Prior to entering the tube bundle area, feedwater returning from the condenser mixes with saturated liquid that has been trapped by the moisture separators in the downcomer. The saturated liquid from the moisture separators also preheats the feedwater. The density of the downcomer liquid is related to its temperature. Unfortunately, downcomer temperature is not a measured plant variable, although feedwater temperature is. To estimate downcomer temperature, a heat balance is performed on the downcomer:

$$\dot{m}_{dc} c_p T_{dc} = \dot{m}_{fw} c_p T_{fw} + (\dot{m}_{dc} - \dot{m}_{fw})\, c_p T_{sat} \quad (52)$$

where
- $\dot{m}_{dc}$ ▲ mass flow rate in rate in downcomer;
- c_p ▲ specific heat capacity of water;
- T_{dc} ▲ temperature of downcomer water;
- $\dot{m}_{fw}$ ▲ mass flow rate of feedwater;
- T_{fw} ▲ temperature of feedwater; and

T_{sat} ≙ saturation temperature of generator pressure.

assuming that the specific heat capacities in equation (52) are approximately equal. Rearranging (52):

$$T_{dc} = \frac{\dot{m}_{fw} T_{fw} + (\dot{m}_{dc} - \dot{m}_{dc})\, T_{sat}}{\dot{m}_{dc}} \quad (53)$$

The feedwater and steam mass flow rates of the steam generator are measured plant variables, but the downcomer mass flow rate is not. The downcomer mass flow rate can be estimated using the Circulation Ratio. The Circulation Ration is a measure of the quantity of water entering the tube bundle section of the steam generator (downcomer flow) compared tot he total feedwater flow. Circulation ratio is defined as:

$$CR = \frac{\textit{Mass Flow Rate Entering the Tube Bundle}}{\textit{Mass Flow Rate of Feedwater}} = \frac{\dot{m}_{dc}}{\dot{m}_{fw}}$$

Typically, the Circulation Ratio decreases from about 25 at lower powers to about 5 for high powers. By estimating the Circulation Ratio for the power level and multiplying it by the feedwater mass flow rate, it is possible to generate a reasonable value for downcomer mass flow rate.

For the conventional instrument, it is assumed that a good estimate of downcomer temperature would be made and used to calculate a constant downcomer density. It turns out that the downcomer temperature is not a very sensitive function of feedwater temperature. For a feedwater flow rate of 20 kg/s, feedwater temperature of 132°C, saturation temperature of 290 °C, and a Circulation Ratio of 20, (corresponding to about 5 percent power), the downcomer temperature is 282°C.

For a feedwater flow rate of 400 kg/s, feedwater temperature of 268°C, saturation temperature of 286°C, and a Circulation Ratio of 5 (corresponding to nearly 100 percent power), the downcomer temperature is 282°C. Clearly, the conventional instrument is capable of using a single value for downcomer liquid density, 747 kg/m^3 based on T_{dc}=282°C.

A smart level instrument could accept feedwater flow rate and feedwater temperature as inputs and, with knowledge of the details of Circulation Ratio as a function of power, calculate an instantaneous downcomer temperature using equation (53). This calculation is performed by the smart instrument in this report.

5.3 Inputs and Outputs

Figures 24 and 25 show block diagrams for the conventional and smart instruments. The conventional instrument's only variable input would be the output from the differential pressure cell. The only output for the conventional instrument is level, L_d. The smart instrument would have the differential pressure cell input as well as the temperature of the feedwater, T_{fw}, the mass flow rate of the feedwater, $\dot{m}_{fw}$, the Circulation Ratio appropriate for the power level, CR, the steam generator pressure, p_{sg}, and the temperature of the reactor building, T_{amb}. The smart instrument would provide two outputs: level, L, and a flooding warning to alert the operator of an approach to flooding in the drain pipe.

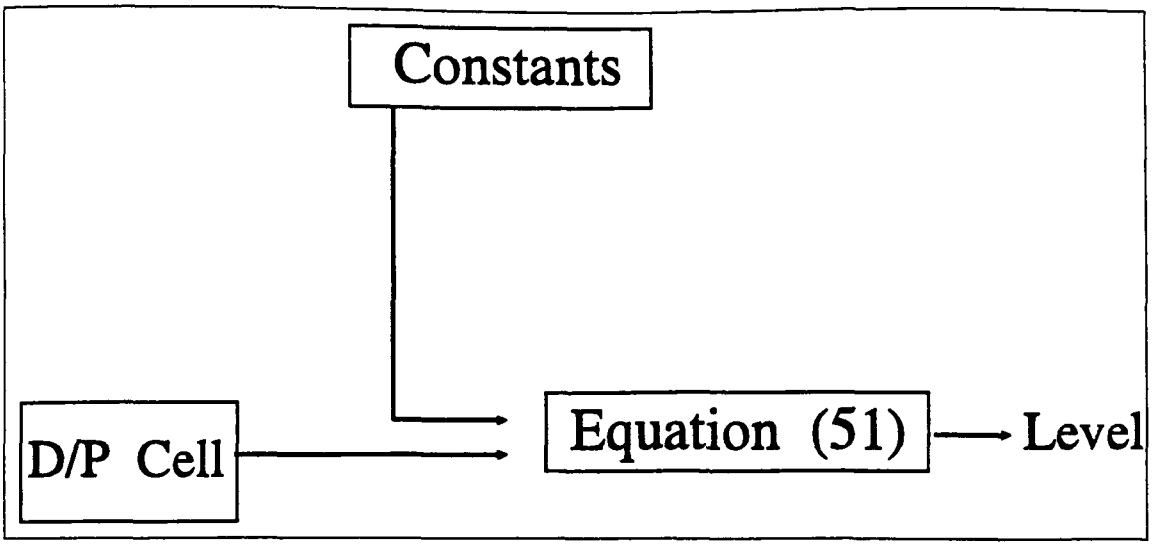

Figure 24: Conventional Level Instrument Block Diagram

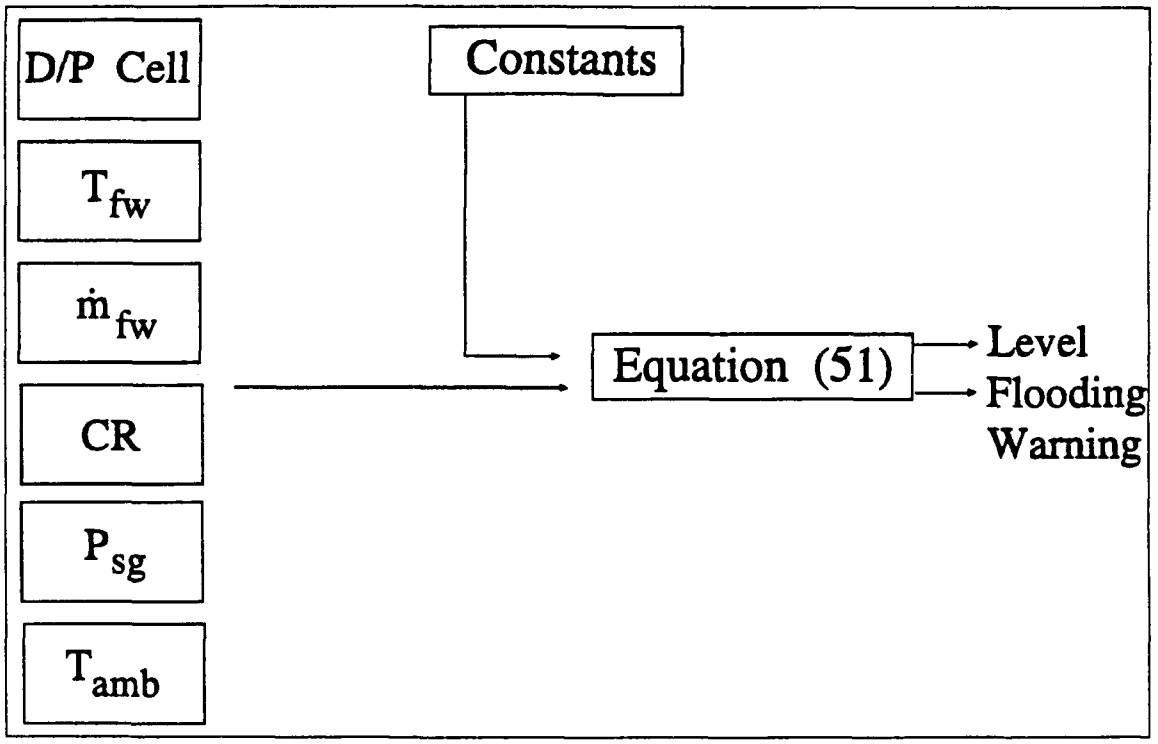

Figure 25: Smart Level Instrument Block Diagram

5.4 Calibration

The output data from the Prism program after running 30 minute simulations of up and down power transients is used to calibrate the conventional and smart instruments. For the purposes of comparison, this procedure assumes that the steam generator data recorded by Prism represents the actual value or truth. The calibration procedure was to compute the downcomer water temperature as a function of time using equation (55), assuming a Circulation Ratio of 5 for the power level, to find the downcomer liquid density, ρ_ℓ, as a function of time, compute the vapor density, ρ_v, as a function of time based on the Prism data for generator pressure, use fixed values of reference leg density, ρ_r=988 kg/m^3, reference leg height, H=2 m, and use the Prism data for generator level to solve equation (1) for the differential pressure cell output, ΔP, as a function of time.

Naturally, using this calculation procedure, it is not instructive to compare the smart level instrument calculated level output with the level signal recorded by Prism. They are identical because the procedure and data used by the smart instrument to calculate steam generator level from differential pressure cell data is just the inverse of the procedure used to derive the differential pressure cell data from the Prism level information.

5.5 Comparison

The time varying differential pressure cell output, $\Delta P(t)$, extracted from Prism data by the procedure described in the previous section, was applied to the simplified calculation (51) performed by the conventional instrument and to the more detailed calculation performed by the smart instrument.

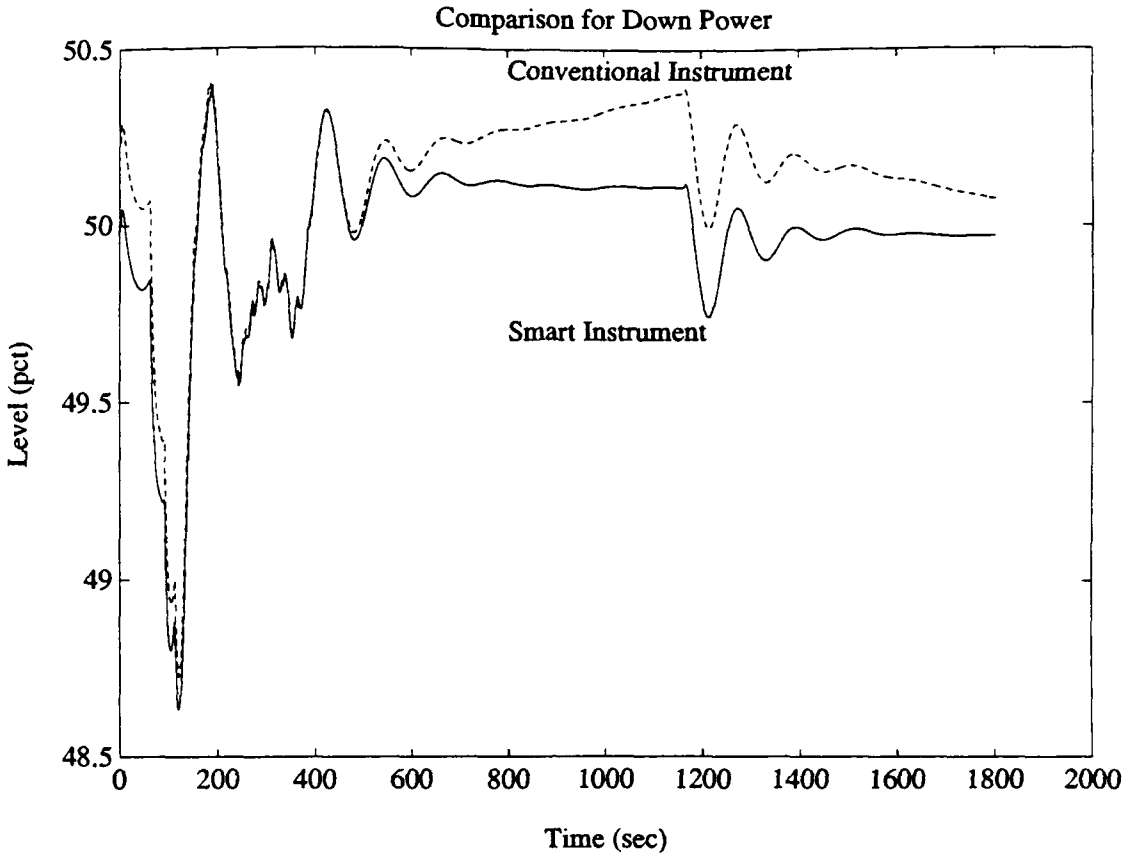

Figure 26: Comparison of Level Signals for Down Power

Figure 26 is plot of the level signals as functions of time for the smart and conventional instruments for a down power from 100 to 90 percent power. Recall that the difference between the two calculated levels is that the conventional instrument uses an average value for vapor density, constant downcomer liquid density, and neglects the differential pressure between the condensing pot and steam generator. The smart instrument calculates the vapor density and liquid density at each time step, and does not neglect the pressure difference between steam generator and condensing pot. Figure 27 show that the level error between the conventional and smart instruments varies, but is generally below .5 percent.

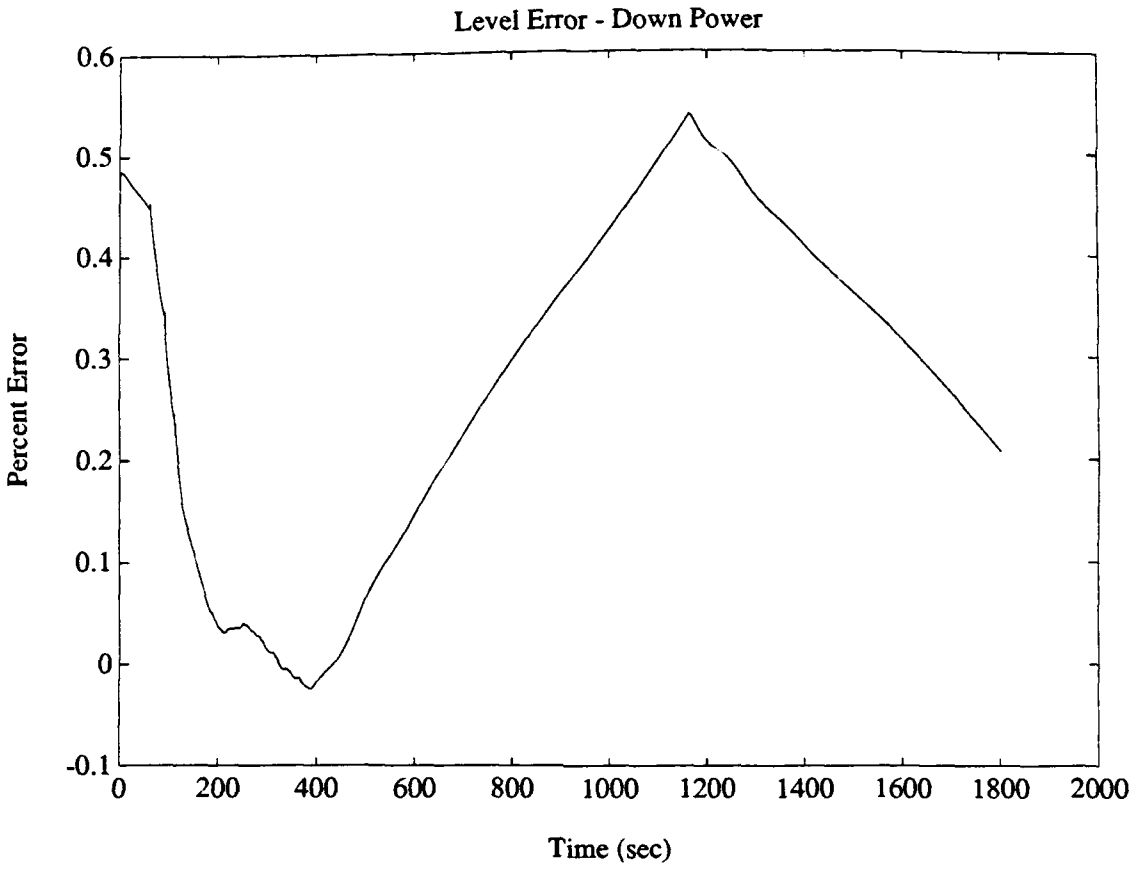

Figure 27: Level Error For Down Power

Figure 28 is a comparison of the level signals for an up power transient from 90 to 100 percent. From figure 29, the minimum deviation between the level signals for the up power is .4 percent, but at no time is the error greater than 1 percent.

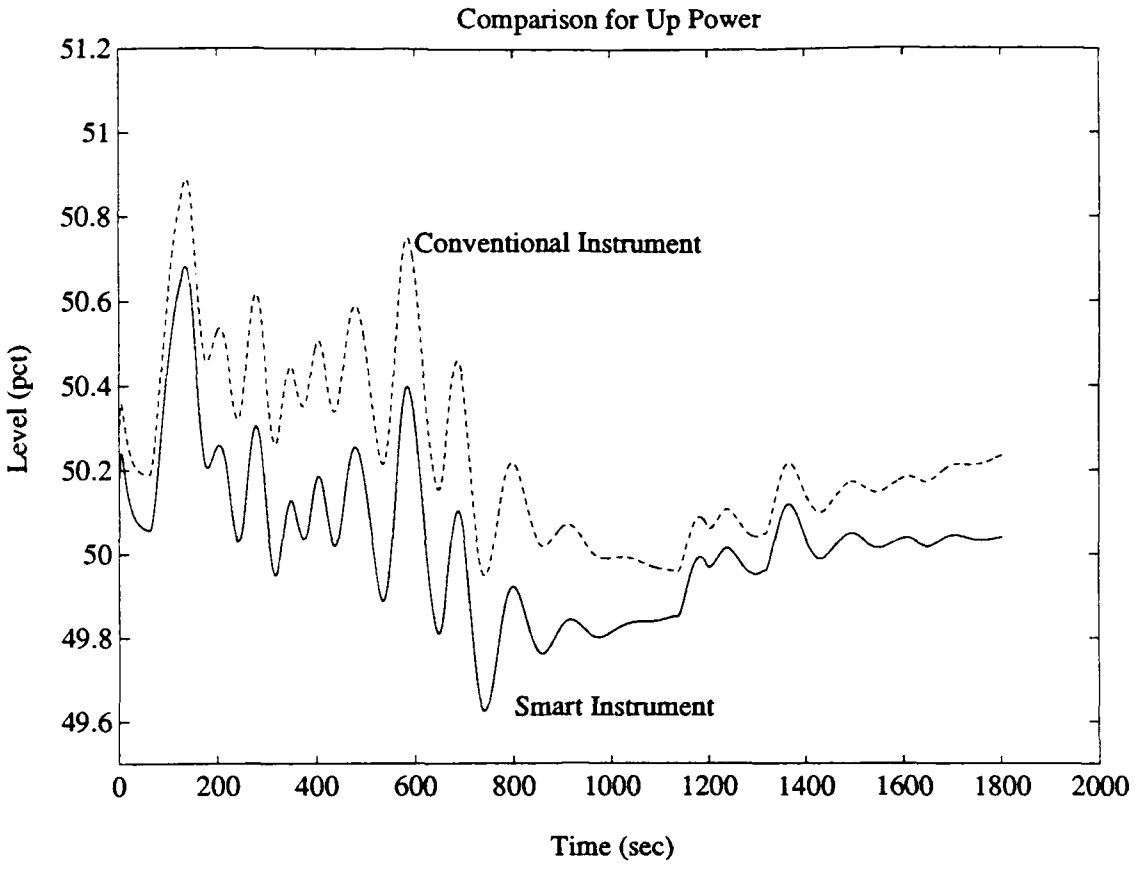

Figure 28: Level Comparison for Up Power

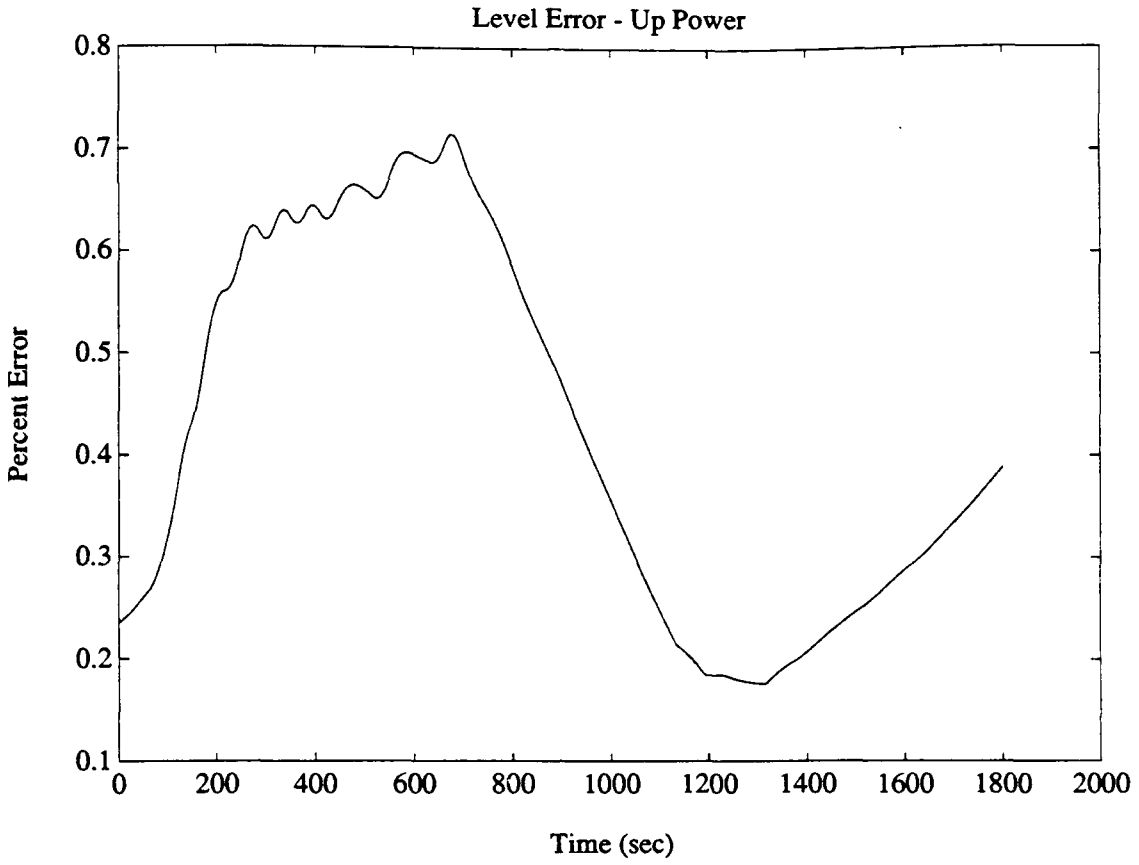

Figure 29: Level Error For Up Power

Conclusions

The operation and accuracy of a smart instrument was investigated. The model was used by the smart instrument was developed in chapter 4. The input variables for the smart instrument are steam generator pressure, feedwater flow rate and temperature, reactor building temperature, Circulation Ratio, and differential pressure cell output. For the basis of comparison, a "conventional" level instrument was developed by analyzing the behavior of the variables in equation (51) over the range of steam generator pressures reasonable during power operation and taking all

quantities in equation (51) constant except for the differential pressure cell output. The only input variable to the conventional instrument is thus differential pressure cell output. Since not operational differential pressure cell data was available, the Prism program was used to generate level information as a function of time for two power transients and the differential pressure cell data for both transients was extracted from the Prism level data. To the extent that the simulated differential pressure signal is valid, the smart instrument was more accurate than the conventional instrument, but the difference between the two level signals over the thirty minutes of simulation never exceeded one percent. It is likely that process noise, normal sensor fluctuations, and meter error would completely obscure such a small accuracy improvement.

Although the smart instrument is not significantly more accurate than the postulated conventional level instrument over the range of pressure changes produced by the small power transients (ten percent) imposed on the Prism program, the smart level instrument is capable of estimating the liquid level in the drain pipe between condensing pot and steam generator while the conventional instrument is not. Thus, the smart instrument, while being only slightly more accurate, is capable of identifying and warning the operator of a violation of the assumption common to both smart and conventional level instruments: that the reference leg height is constant. While a utility's response to a smart instrument reporting that drain pipe flooding during power operations would no doubt be exactly the same as if a conventional level instrument's output produced unexpected jumps in level characteristic of drain pipe flooding (i.e., replace the drain pipe or condensing pot with different size piping), the smart instrument's ability to infer variables not easily measured and take action based on that

information has been demonstrated.

Chapter 6

Conclusions

A procedure for designing and implementing a smart instrument was applied to a Pressurized Water Reactor steam generator water level measurement. Important physical effects on generator level were considered and applied to find an overall model capable of inferring desired variables that are not directly measured. The model is stable for constant steam generator pressure and is also stable for a limited range of steam generator pressure transients. A conventional level instrument, using a simplified procedure to calculate level, was chosen for comparison with the smart level instrument. Both instruments received differential pressure cell data extracted from Prism level for two transients. As expected for this comparison, the smart instrument output conformed more closely to the "true" steam generator level, but the difference between the smart instrument and the conventional instrument was never more than 1 percent.

6.1 Significance of Corrections

To understand why there was so little difference between the smart instrument level data and the conventional instrument data, it is necessary to compare the magnitude of the corrections made by the smart instrument to the differential pressure signal.

The differential pressure cell output extracted from Prism output data is on the order of 365 kPa. The maximum steam

generator to condensing pot pressure difference calculated was 1 kPa. Clearly, it is safe to conclude that the differential pressure is negligible.

The smart instrument calculates the downcomer temperature and uses this temperature to adjust the liquid density in the downcomer at each time step. The conventional instrument uses a constant downcomer temperature of 282°C. The range of downcomer temperatures calculated by the smart instrument is 280°C (ρ_ℓ=750 kg/m^3) to 282°C (ρ_ℓ=747 kg/m^3). This small variation in downcomer temperature produces a variation in liquid density of only 0.49 percent.

The steam generator pressure changes for both the up and down powers were on the order of 100 kPa from a nominal steam generator pressure of 7 MPa. This pressure deviation results in a maximum vapor density difference over the entire maneuver of 1.6 percent.

Originally, the temperature of the reactor building was intended to be an input to the smart instrument since it seemed plausible that a steam leak in the reactor building would significantly raise the ambient temperature in the vicinity of the reference leg, thus decreasing the density of the liquid in the reference leg. Indeed, a steam leak that raised the reactor building temperature from 50°C to 200°C would change the density of the reference leg from 988 kg/m^3 to 865 kg/m^3, a change of 12.5 percent. However, the magnitude of the differential pressure cell output, ΔP in equation (51), dominates the value of computed level so the resulting effect on generator level of a reactor building temperature change of this magnitude would be only .7 percent. A steam leak into the reactor building would significantly raise the ambient humidity, making all instrumentation suspect of erratic operation and place the

plant at risk of uncovering the core. Under the circumstances, a .7 percent change in indicated steam generator level would not be as important as the other effects on the reactor plant.

Obviously, none of the simplifications and assumptions made by the conventional instrument envisioned for comparison with the smart instrument produce an error in excess of 1.6 percent. This small deviation from the "true" steam generator level is really too small for the operators to notice, so the smart instrument measuring steam generator level does not provide a realistic increase in indication accuracy. It still would be useful for warning the operator of the approach to a flooding situation in the drain pipe.

6.2 Smart Instrument Design

This research indicates there are several considerations to observe when designing a smart instrument:

- select the variables for measurement;

- choose a model that incorporates as much detail about the physical process as necessary to achieve the measurement accuracy desired and the computational resources of available microprocessors;

- evaluate the model stability and accuracy of results;

- compare the smart instrument with a conventional instrument to evaluate the magnitude of the accuracy improvement;

- compare information available to the operator using the conventional instrument to that provided by the

smart instrument, even if not significantly more accurate, the designer may still opt for the smart instrument because of the extra information it provided.

6.3 Flooding

The suggested model describing steam generator level dynamics, to the extent it closely approximates the actual variables involved, is capable of calculating the liquid level in the drain pipe between the steam generator and the condensing pot directly. By observing when the liquid level reaches or almost reaches the top of the drain pipe, the smart level instrument envisioned by this research could warn the operator that its level output data is on the verge of unreliability. It is important to note, that the ability of the smart instrument to compute a solution of equation (49) for the state variables is predicated on the condition that flooding in the drain pipe does not occur, since equations (28) and (29), used to relate the liquid height in the drain pipe and the pressure gradient between the condensing pot and steam generator to the superficial velocities in the pipe, are not valid after flooding occurs. The pertinent question then is how does the smart instrument recover from just such a flooding condition since its model is now no longer valid?

To recover from a flooding condition, the smart instrument should be programmed with a routine to estimate the steam generator water level based on the reduced reference leg height discussed in section 4.1 and depicted in figure 5. The instrument should warn the operator that flooding has occurred, but still be able to present its best estimate for water level. Next, the routine used to find the superficial velocities from the tables that have been pre-computed must

be capable of responding to the case when the input arguments, liquid height in the drain pipe and pressure gradient, fall outside the bounds of the tabular data. The smart instrument should then try to calculate level after discarding its prior data, in effect re-zeroing itself. It should continue to zero itself and try to calculate transient values of the state variables until the a the drain pipe liquid level is reduced and the pipe is no longer flooded.

Conclusions

This research discusses how and why smart instruments might be applied to nuclear power plants. The features that distinguish a smart instrument from a conventional instrument are a process model and the ability of the smart instrument to make decisions based on plant variables and model output. A good model of the physical process enables the instrument to monitor measurement results and warn the user if the data received is not consistent with redundant sensors or trends indicated by sensors for different variables. The important issues to consider when designing a smart instrument were explored and actually illustrated by a specific example: design of a smart instrument for steam generator water level measurement. A model of steam generator level variations as a function of power was proposed to reduce the number of assumptions necessary for level computation and to infer unmeasured variables germane to the reliability of the remaining assumptions. The Prism program was used to generate simulated level data, from which an estimated differential pressure cell output signal was extracted. The differential pressure cell signal and other Prism data were input to the smart level instrument. The "smart" level produced was compared to a conventional level instrument's output. The smart level signal was only

marginally more accurate than the conventional level signal but the smart instrument is capable of inferring important variables that the conventional instrument cannot. Finally, the smart instrument must be capable of recovering from brief operation outside the limits of its model, otherwise the designer risks that certain transients could render the instrument's subsequent output unreliable.

Chapter 7

Recommendations for Future Work

There has not been sufficient time during the term of this research to pursue all the issues involved in smart instrumentation implementation as thoroughly as desired. Topics related to a smart level instrument worthy of additional investigation include: determining the criteria affecting the theoretical stability of the one-step, implicit difference equation (equation (48)) used to compute the solution to the linearized equations, investigating model behavior at lower steam generator pressures, numerically analyzing of the solution method, and obtaining experimental data on flow transitions and pipe liquid height for two phase counter-current flow and comparing the experimental results to the predicted results. Applying the design methodology suggested in this research or another method to the measurement and display of other nuclear reactor plant variables, such as reactivity measurement and control, would be of interest for the continued study of smart instruments in general.

7.1 Theoretical Stability

Before implementing the proposed model for steam generator level measurement, the specific conditions for stability of equation (24), the general differential equation, and equation (48) the one-step implicit difference, should be determined.

7.2 Operation at Lower Pressures

The steam generator level model developed in this research was only applied to level measurement at normal steam generator operating pressure, about 7.0 to 7.6 MPa. For the smart instrument to really replace conventional level instruments, it must be capable of operating over the entire range of generator pressures encountered in practice, extending down to atmospheric pressure. To investigate model performance at other pressures, solutions to the momentum balance equations, (28) and (29), must be computed for several pressures between 7.6 MPa and atmospheric since the liquid and vapor densities, taken as constants when iteratively solving equations (28) and (29), are strong functions of pressure in the steam generator.

7.3 Physical Testing

As the comparison of results in Chapter 5 illustrated, the smart level instrument employing a detailed model was only marginally more accurate than a conventional level instrument using a simplified model. Still, the smart instrument is capable of calculating the transient liquid level in the drain pipe and can therefore detect the onset of flooding in the drain pipe and subsequent erroneous level indication. Since the ability to predict the drain pipe liquid level is the distinguishing feature of the smart instrument, the accuracy of the prediction should be evaluated by physical experiment. The physical data obtained could be used to improve the model used as well.

7.4 Numerical Analysis

Computing the solution to equation (48) is very time consuming. The solution for the positive pressure ramps requires several hours to complete on a DECstation 3100, a particularly fast workstation. It would be potentially

beneficial to further analyze the equations involved and construct an algorithm designed to enhance the speed of the solution. Certainly, the speed of the calculations could be significantly enhanced by the use of a compiled high level computer language for the computations.

7.5 Application to Other Variables

The application of smart instruments to measurement and control of other nuclear power plant variables should be investigated. In addition to evaluating and displaying the value of a simple plant variable, use with complicated systems like reactivity or steam generator water level control should be explored. A smart instrument could be a key component of an expert system used for power plant operation and casualty control. The smart instrument could be responsible for redundancy and consistency checks while an external computer evaluates the over all system, postulates probable outcomes to certain actions, and can recommend corrective action. Specific applications utilizing the ability of smart instruments to communicate with each other should also be explored. Sensors could be networked together and either polled by a control system or signal the control system when they have data to transmit.

References

[C1] Chow, V.T., *Open Channel Flow Theory*, McGraw Hill Book Company, NY, 1959.

[C2] Collier, J.G., *Convective Boiling and Condensation*, 2nd ed, McGraw Hill, NY, 1981.

[G1] Garner, G.M., *Fault Detection and Level Validation in Boiling Water Reactors*, MIT Phd Thesis, CSDL-T-858, Sep 1985

[K1] Kao, S.P., "Prism: An Integrated RCS and Steam Generator Simulation," *ANS Topical Meeting on Advances in Mathematical Computations and Reactor Physics*, 29 Apr-2 May 1991, Pittsburgh, PA.

[L1] Lopez de Bertodano, M.A., *Fast Numerical Methods for Two Phase Situations in Nuclear Reactors*, MIT Engineer Thesis, 1983.

[L2] Lumley, J.L.,Van Dyke, M., co-editors, *Annual Review of Fluid Mechanics*, Vol 23, Annual Reviews, Inc., Palo Alto, 1991.

[M1] McAdams, *Heat Transmission*, McGraw Hill, NY, 1954.

[M2] Meyjer, C.H., Pasquenza, J.P., Deckert, J.C., Fisher, J.L., Lanning, D.B., Ray, A., *On-Line Power Plant Signal Validation Technique Utilizing Parity-Space Representation and Analytic Redundancy*, Electric Power Research Institute, Palo Alto, CA, Nov 1981, NP-2110.

[M3] Mische, G., *Systems Summary of a Westinghouse Pressurized Water Reactor Nuclear Power Plant*, Westinghouse Electric Corporation, 1971.

[P1] "Pro-Matlab Version 3.5c," The Mathworks, Inc., S. Natick, MA, May 1990.

[R1] Rahn, F.J., Adamantiades, A.G., Kenton, J.E., Braun, C, *A Guide To Nuclear Power Technology*, John Wiley and Sons, New York, 1984.

[R2] Rogers and Mayhew, *Engineering Thermodynamic Work and Heat Transfer*, Longmans, London, 1980.

[S1] Swisher, V.I., "User's Guide For Signal Validation Software," Electric Power Research Institute, Sep 1987, NP-5389.

[T1] Taitel, Y., and Dukler, A.E., "A Model for Predicting Flow Transitions in Horizontal and Near Horizontal Gas-Liquid Flow," *American Institute of Chemical Engineering Journal* (Vol 22 Nr 1), Jan 1976, p. 47-55.

[T2] Todreas and Kazimi, *Nuclear Systems I*, Hemisphere Publishing Corp, NY, 1990.

[W1] Wallis, G.B., *One-Dimensional Two-Phase Flow*, McGraw Hill Book Co., NY, 1969.

Bibliography

Chow, V.T., *Open Channel Flow Theory*, McGraw Hill Book Company, NY, 1959.

Collier, J.G., *Convective Boiling and Condensation*, 2nd ed, McGraw Hill, NY, 1981.

Douglas, *Fluid Mechanics*, 1979, Pitman Publishing, Ltd., London.

Garner, G.M., *Fault Detection and Level Validation in Boiling Water Reactors*, MIT Phd Thesis, CSDL-T-858, Sep 1985.

Kao, S.P., "Prism: An Integrated RCS and Steam Generator Simulation," *ANS Topical Meeting on Advances in Mathematical Computations and Reactor Physics*, 29 Apr-2 May 1991, Pittsburgh, PA.

Kays, W.M., London, A.L., *Compact Heat Exchangers*, The National Press, Palo Alto, 1955.

Keenan, J.H. et al., *Steam Tables (Metric Units)*, John Wiley and Sons, NY, 1969.

Lopez de Bertodano, M.A., *Fast Numerical Methods for Two Phase Situations in Nuclear Reactors*, MIT S.M. Thesis, 1983.

Lumley, J.L.,Van Dyke, M., co-editors, *Annual Review of Fluid Mechanics*, Vol 23, Annual Reviews, Inc., Palo Alto, 1991.

Massey, B.S., *Mechanics of Fluids*, Van Nostrand Reingold

Co., Ltd, Berkshire, England, 1983.

McAdams, *Heat Transmission*, McGraw Hill, NY, 1954.

Mische, G., *Systems Summary of a Westinghouse Pressurized Water Reactor Nuclear Power Plant*, Westinghouse Electric Corporation, 1971.

Olson, R.M., *Essentials of Fluid Mechanics*, Harper and Row, NY, 1973.

Rahn, F.J., Adamantiades, A.G., *A Guide To Nuclear Power Technology*, John Wiley and Sons, New York, 1984.

Rogers and Mayhew, *Engineering Thermodynamic Work and Heat Transfer*, Longmans, London, 1980.

Taitel, Y., and Dukler, A.E., "A Model for Predicting Flow Transitions in Horizontal and Near Horizontal Gas-Liquid Flow," *American Institute of Chemical Engineering Journal* (Vol 22 Nr 1), Jan 1976, p. 47-55.

Todreas and Kazimi, *Nuclear Systems I*, Hemisphere Publishing Corp, NY, 1990.

Wallis, G.B., *One-Dimensional Two-Phase Flow*, McGraw Hill Book Co., NY, 1969.

Welty, J.R., *Engineering Heat Transfer*, John Wiley and Sons, NY, 1974.

Appendix

The PRO-MATLAB program, numerical processing software based on LINPACK and EISPACK codes, is used to solve equation (48) for each of the postulated transients. PRO-MATLAB is an optimized program that is well-suited for high speed calculations on large matrices and vectors. The program is capable of processing commands that have been saved to a text file, called a macro, and allows the user to create his own functions. Neither functions or macros are compiled, but they were used to develop prototype algorithms to compute solutions to equation (48). The same routines could be compiled and used by the smart level instrument to perform similar calculations. The matlab macros and functions used are included in the following pages.

```
%macro to start calculating a solution to equation (48)
stmdat
%gets rhol_list, rhov_list,Hl_list,Hv_list,pressure
variables
%gets table_h and table_press values (for jv and jl data),
jvdat and jldat
dt=1*.5;
L=2.5;%length of drain pipe
Dt=.0254;%drain pipe dia
Dc=2*.0254;%condensing pot dia
Lc=3.5*2.54e-2;%length of condensing pot
dpdx=-73.27493046894671;
startpsg=7.34e6;
endpsg=7.0400e6;%
stoptrans=225/dt;
minutes=4;%number of minutes to simulate
input=[startpsg+dpdx*L;.71227377;0.00546943];

deltas=[-30;.001;.0005];%deltas to use in computing
derivatives
X_=[];
f_=[];
prsg=[];
%X is the set of intermediate values of the result for each
time %step
for n=-5/dt:minutes*60/dt
 %controls psg(t)->
 if n<=0
  psg=startpsg;%initial value
 elseif n<stoptrans+1
  psg=startpsg-n*(startpsg-endpsg)/stoptrans;%for ea time
%step during power chg
 else
  psg=endpsg;
 end
X_=[X_ input];
prsg=[prsg; psg];
psg
% display dp/dx and dp/dx + dp
 (input(1)-psg)/L
 (input(1)-psg)/L+deltas(1)
 [X,f]=solveit(psg,70000,dt,input,L,Dc,Dt,Lc,deltas,...
jvdat,jldat,rhol_list,rhov_list,Hl_list,Hv_list,...
table_press,table_h,pressure);
 input=X;
 disp('finished time step')
 n*dt
 f_=[f_ f];
end
```

```
%this is the macro stmdat
%get steam table data in flat file form
load stmdata.prn
n=16;%number of pressure data pairs
pressure=stmdata(1:n);
rhol_list=ones(1:n)'./stmdata(n+1:2*n);
rhov_list=ones(1:n)'./stmdata(2*n+1:3*n);
Hl_list=stmdata(3*n+1:4*n);
Hv_list=stmdata(4*n+1:5*n);
%load outdata3.prn
load outdata4.prn
n1=41;%number of pressure data pairs
table_h=[0;.001;.0015;.002;.0025;.003;.0035;.004;.008;...
.012;.016;.020;.023;025];%order of liquid heights

table_press=[600;570;540;510;480;450;420;390;360;330;300;...
270;240;210;180;150;120;90;60;30;0;-30;-60;-90.1;-120.1;...
-150.1;-180.2;-210.2;-240.2;-270.2;-300.3;-330.3;-360.3;...
-390.3;-420.4;-450.4;-480.4;-510.4;-540.5;-570.5;-600.5];

jvdat=outdata4(1:14*n1);
jldat=outdata4(14*n1+1:28*n1);
end
```

```
function [X,f] =solveit(psg,dpsg,dt,inputx,L,Dc,Dt,Lc,...
d,jvdat,jldat,rhol_list,rhov_list,Hl_list,Hv_list,...
table_press,table_h,pressure);
%function to solve the equation and compile the answers

%psg is initial generator pressure
%dpsg is delta generator pressure
%dt is time interval of manuever
%inputx is inputx=[pc;alpha_c;h]
%L is length of drain pipe
%Dc is condensing pot diameter
%Dt is drain pipe diameter
%d is deltas of x variables for numerical differentiation
%d=[dpc;dalpha_c;dh] [-30;.0005;.0005]
%you get jvdat,jldat, rhol_list, rhov_list, Hl_list,
Hv_list,table_press,
%table_h from running stmdat
%pressure is the list of pressures for which steam table
data is available in
%the file stmdata.prn read by stmdat.m

%define  given deltas to use for numerical derivatives
dp=d(1);
da=d(2);
dh=d(3);
%
%for n=1:5

%  psg=psg-n*dpsg/600;%for each time step
%define state variables
  alpha_c=inputx(2);
  pc=inputx(1);
  hl=inputx(3);
  %now build the df/dx vector
df11=first(alpha_c,psg,pc,hl,L,Dc,Dt,dp,jvdat,jldat,...
table_press,table_h);
df12=second(alpha_c,psg,pc,hl,L,Dc,Dt,da,jvdat,jldat,...
table_press,table_h);
df13=third(alpha_c,psg,pc,hl,L,Dc,Dt,dh,jvdat,jldat,...
table_press,table_h);
df21=fourth(alpha_c,psg,pc,hl,L,Dc,Dt,dp,jvdat,jldat,...
table_press,table_h);
df22=fifth(alpha_c,psg,pc,hl,L,Dc,Dt,da,jvdat,jldat,...
table_press,table_h);
df23=sixth(alpha_c,psg,pc,hl,L,Dc,Dt,dh,jvdat,jldat,...
table_press,table_h);
df31=seventh(alpha_c,psg,pc,hl,L,Dc,Dt,dp,jvdat,jldat,...
table_press,table_h);
df32=eighth(alpha_c,psg,pc,hl,L,Dc,Dt,da,jvdat,jldat,...
table_press,table_h);
df33=ninth(alpha_c,psg,pc,hl,L,Dc,Dt,dh,jvdat,jldat,...
table_press,table_h);
```

```
df=[df11 df12 df13;df21 df22 df23;df31 df32 df33];
  %
  %get the f vector
  f=findf(alpha_c,psg,pc,hl,Dc,Dt,L,jvdat,jldat,...
  table_press,table_h)
  %
  %get the A vector
  %
  A=buildA (pc,alpha_c,hl,rhol_list,rhov_list,Hl_list,...
  Hv_list,Dc,Dt,L,Lc,pressure);

  X=inv((A/dt - df))*f + inputx;

disp('finished time step')

end
```

```
function [df1dpc]=first
(alpha_c,psg,pc,hl,L,Dc,Dt,dp,jvdat,jldat,press,givenh)
%
%function to compute the derivative of f1 wrt pc
%
%functions first.m through ninth.m use similar arguments:
%
%alpha_c is the vapor volume fraction in the condensing pot
%psg is the steam generator pressure
%pc is the condensing pot pressure
%hl is the liquid height in the drain pipe
%L is the length of the drain pipe
%Dc is the diameter of the condensing pot (a horiz cylinder)
%Dt is the diameter of the drain pipe
%dp or da or dh are the deltas used to compute the
derivatives %wrt
%pc,alpha_c, or hl
%press and givenh are the P' and h data used to compute the
jvdat %and jldat
%tables


theta=.0164;
%

%get steam data
[a,b,Tsat,mu,k,rhov1,rhol] = stminfo (pc);
[a,b,Tsat,mu,k,rhov2,rhol] = stminfo (pc+dp);
%
%find mdot
%
mdotw1 = findmdot(alpha_c,Dc,Dt,pc,theta);
mdotw2 = mdotw1;%same as
mdotw2=findmdot(alpha_c,Dc,Dt,pc+dp,theta);
%
%find jv
%
[jl1 jv1] =
findjvjl(hl,(pc-psg)/L,givenh,press,jvdat,jldat);
[jl2 jv2] =
findjvjl(hl,(pc-psg)/L+dp,givenh,press,jvdat,jldat);
%
A=(Dt/2)^2*pi;%area of pipe
%f1=rhov1*jv1*A-mdotw1
df1dpc = ((rhov2*jv2*A - mdotw2)-(rhov1*jv1*A - mdotw1))/dp;
end
```

```
function[df1dac]=second(alpha_c,psg,pc,hl,L,Dc,...
Dt,da,jvdat,jldat,press,givenh)
%
%function to compute the derivative of f1 wrt alpha_c
%
%function [df1dac] = second
(alpha_c,psg,pc,hl,Dc,Dt,da,jvdat,jldat)
%
theta=.0164;


%get steam data
[a,b,Tsat,mu,k,rhov1,rhol] = stminfo (pc);
%
%find mdot
%
mdotw1 = findmdot(alpha_c,Dc,Dt,pc,theta);
mdotw2 = findmdot(alpha_c+da,Dc,Dt,pc,theta);

%
%find jv
%
[jl1 jv1] =
findjvjl(hl,(pc-psg)/L,givenh,press,jvdat,jldat);
[jl2 jv2] =
findjvjl(hl,(pc-psg)/L,givenh,press,jvdat,jldat);
%
A=(Dt/2)^2*pi;%area of pipe
%f1=rhov1*jv1*A-mdotw1;
df1dac = ((rhov1*jv2*A - mdotw2)-(rhov1*jv1*A - mdotw1))/da;
end
```

```
function[df1dh]=third(alpha_c,psg,pc,hl,L,Dc,...
Dt,dh,jvdat,jldat,press,givenh)
%
%function to compute the derivative of f1 wrt h
%
%function [df1dpc] = third
(alpha_c,psg,pc,hl,L,Dc,Dt,dh,jvdat,jldat)

theta=.0164;
%

%get steam data
[a,b,Tsat,mu,k,rhov1,rhol] = stminfo (pc);
%
%find mdot
%
mdotw1 = findmdot(alpha_c,Dc,Dt,pc,theta);
%
%find jv
%
[jl1 jv1] =
findjvjl(hl,(pc-psg)/L,givenh,press,jvdat,jldat);
[jl2 jv2] =
findjvjl(hl+dh,(pc-psg)/L,givenh,press,jvdat,jldat);
%
A=(Dt/2)^2*pi;%area of pipe

df1dh = ((rhov1*jv2*A - mdotw1)-(rhov1*jv1*A - mdotw1))/dh;
end
```

```
function[df2dpc]=fourth(alpha_c,psg,pc,hl,L,Dc,Dt,...
dp,jvdat,jldat,press,givenh)
%
%function to compute the derivative of f2 wrt pc
%
%function [df1dpc] = fourth
(alpha_c,psg,pc,hl,Dc,Dt,dp,jvdat,jldat)

theta=.0164;
%

%get steam data
[Hl1,Hv1,Tsat,mu,k,rhov1,rhol] = stminfo (pc);
[Hl2,Hv2,Tsat,mu,k,rhov2,rhol] = stminfo (pc+dp);
%
%find mdot
%
mdotw1 = findmdot(alpha_c,Dc,Dt,pc,theta);
mdotw2 = mdotw1;% same as
mdotw2=findmdot(alpha_c,Dc,Dt,pc+dp,theta);
%
%find jv
%
[jl1 jv1] =
findjvjl(hl,(pc-psg)/L,givenh,press,jvdat,jldat);
[jl2 jv2] =
findjvjl(hl,(pc-psg)/L+dp,givenh,press,jvdat,jldat);
%
%findQ
%
Q1=findQ(pc);
Q2=findQ(pc+dp);
A=(Dt/2)^2*pi;%area of pipe
f2=rhov1*jv1*Hv1*A-mdotw1*Hl1-Q1;
df2dpc =
((rhov2*jv2*Hv2*A-mdotw2*Hl2-Q2)-(rhov1*jv1*Hv1*A-mdotw1*Hl1
-...
Q1))/dp;
end
```

```
function[df2dac]=fifth(alpha_c,psg,pc,hl,L,Dc,Dt,...
da,jvdat,jldat,press,givenh)
%
%function to compute the derivative of f2 wrt alpha_c
%

theta=.0164;
%

%get steam data
[Hll,Hv1,Tsat,mu,k,rhov1,rhol] = stminfo (pc);
%
%find mdot
%
mdotw1 = findmdot(alpha_c,Dc,Dt,pc,theta);
mdotw2 = findmdot(alpha_c+da,Dc,Dt,pc,theta);
%
%find jv
%
[jl1 jv1] =
findjvjl(hl,(pc-psg)/L,givenh,press,jvdat,jldat);

%
%findQ
%
Q1=findQ(pc);

A=(Dt/2)^2*pi;%area of pipe
%f2=rhov1*jv1*Hv1*A-mdotw1*Hl1-Q1
df2dac =
((rhov1*jv1*Hv1*A-mdotw2*Hl1-Q1)-(rhov1*jv1*Hv1*A-mdotw1*Hl1
-...
Q1))/da;
end
```

```
function[df2dh]=sixth(alpha_c,psg,pc,hl,L,Dc,Dt,...
dh,jvdat,jldat,press,givenh)
%
%function to compute the derivative of f2 wrt h
%
%function    [df1dh] = third
(alpha_c,psg,pc,hl,Dc,Dt,dh,jvdat,jldat)

theta=.0164;
%

%get steam data
[Hl1,Hv1,Tsat,mu,k,rhov1,rhol] = stminfo (pc);
%
%find mdot
%
mdotw1 = findmdot(alpha_c,Dc,Dt,pc,theta);

%
%find jv
%
[jl1 jv1] =
findjvjl(hl,(pc-psg)/L,givenh,press,jvdat,jldat);
[jl2 jv2] =
findjvjl(hl+dh,(pc-psg)/L,givenh,press,jvdat,jldat);
%
%findQ
%
Q1=findQ(pc);
A=(Dt/2)^2*pi;%area of pipe
f2=rhov1*jv1*Hv1*A-mdotw1*Hl1-Q1;
df2dh =
((rhov1*jv2*Hv1*A-mdotw1*Hl1-Q1)-(rhov1*jv1*Hv1*A-mdotw1*Hl1
...
-Q1))/dh;
end
```

```
function[df3dpc]=seventh(alpha_c,psg,pc,hl,L,Dc,Dt,...
dp,jvdat,jldat,press,givenh)
%
%function to compute the derivative of f3 wrt pc
%

theta=.0164;
%

%get steam data
[a,b,Tsat,mu,k,rhov1,rhol1] = stminfo (pc);
[a,b,Tsat,mu,k,rhov2,rhol2] = stminfo (pc+dp);
%
%find mdot
%
mdotw1 = findmdot(alpha_c,Dc,Dt,pc,theta);
mdotw2 = findmdot(alpha_c,Dc,Dt,pc+dp,theta);
%
%find jv
%
[jl1 jv1] =
findjvjl(hl,(pc-psg)/L,givenh,press,jvdat,jldat);
[jl2 jv2] =
findjvjl(hl,(pc-psg)/L+dp,givenh,press,jvdat,jldat);
%
A=(Dt/2)^2*pi;%area of pipe
f3=rhol1*jl1*A+mdotw1;
df3dpc = ((rhol2*jl2*A + mdotw2)-(rhol1*jl1*A + mdotw1))/dp;
end
```

```
function [df3dac]=eighth (alpha_c,psg,pc,hl,L,Dc,Dt,da,...
jvdat,jldat,press,givenh)
%
%function to compute the derivative of f3 wrt alpha_c
%

theta=.0164;
%

%get steam data
[a,b,Tsat,mu,k,rhovl,rholl] = stminfo (pc);
%
%find mdot
%
mdotw1 = findmdot(alpha_c,Dc,Dt,pc,theta);
mdotw2 = findmdot(alpha_c+da,Dc,Dt,pc,theta);
%
%find jv
%
[jl1 jv1] =
findjvjl(hl,(pc-psg)/L,givenh,press,jvdat,jldat);
[jl2 jv2] =
findjvjl(hl,(pc-psg)/L,givenh,press,jvdat,jldat);
%
A=(Dt/2)^2*pi;%area of pipe
%f3=rholl*jl1*A+mdotw1;
df3dac = ((rholl*jl2*A + mdotw2)-(rholl*jl1*A + mdotw1))/da;
end
```

```
function[df3dh]=ninth(alpha_c,psg,pc,hl,L,Dc,Dt,...
dh,jvdat,jldat,press,givenh)
%
%function to compute the derivative of f3 wrt h
%

theta=.0164;
%

%get steam data
[a,b,Tsat,mu,k,rhovl,rholl] = stminfo (pc);
%
%find mdot
%
mdotwl = findmdot(alpha_c,Dc,Dt,pc,theta);
%
%find jv
%
[jll jvl] =
findjvjl(hl,(pc-psg)/L,givenh,press,jvdat,jldat);
[jl2 jv2] =
findjvjl(hl+dh,(pc-psg)/L,givenh,press,jvdat,jldat);
%
A=(Dt/2)^2*pi;%area of pipe

df3dh = ((rholl*jl2*A + mdotwl)-(rholl*jll*A + mdotwl))/dh;
end
```

```
function[f]=findf(alpha_c,psg,pc,hl,Dc,Dt,...
L,jvdat,jldat,press,givenh)
%function to compute the f vector
%
%alpha_c is the vapor volume fraction in the condensing pot
%psg is steam generator pressure
%pc is condensing pot pressure
%hl is liquid height in drain pipe
%Dc is condensing pot diameter (a horiz cylinder)
%Dt is drain line diameter
%L is length of drain line
%press and givenh are the P' and h data used to compute the
jvdat %and jldat
%tables


%constants
theta=.0146;
%
%get steam data
[Hl,Hv,Tsat,mu,k,rho_v,rho_l]=stminfo(pc);
%
%find mdot
%
mdotw = findmdot(alpha_c,Dc,Dt,pc,theta);
%
%find jv,jl
[jl jv] = findjvjl(hl,(pc-psg)/L,givenh,press,jvdat,jldat);
%
%find Q
Q=findQ(pc);
%
A=(Dt/2)^2*pi;%area of pipe
%
%find f1
f1=rho_v*jv*A-mdotw;
%
%find f2
f2=rho_v*jv*Hv*A-mdotw*Hl-Q;
%
%find f3
f3=rho_l*jl*A+mdotw;
%
f=[f1;f2;f3];
end
```

```
function[A]= buildA(pc,alpha_c,hl,rhol_list,rhov_list,...
Hl_list,Hv_list,Dc,Dt,Lt,Lc,pssr)
%
%function that builds the A matrix, xxx_list are the stm
table %lists of
%data for the pressures read in from stmdata.prn by stmdat.m
%pssr is the range of pressures used to extract steam table
data
%
%pc is pressure in condensing pot
%alpha_c is vapor volume fraction in condensing pot
%hl is liquid hight in the drain pipe
%Lt is the length of the drain pipe
%Lc is the length of the condensing pot (assumed to be a
horiz %cylinder)
%
%uses:      1. stminfo.m
%           2. deriv.m
%

Vc=(Dc/2)^2*pi*Lc;%volume of condensing pot
[Hl Hv Tsat mu k rhov rhol]=stminfo(pc);%stm table info
%
%note: deriv(pssr,rhol_list,pc,.01) computes the partial
deriv of %rhol wrt pc at pc

%compute a11
a11=((1-alpha_c)*deriv(pssr,rhol_list,pc,.01)+alpha_c*...
(deriv(pssr,rhov_list,pc,.01)))*Vc;
%
%compute a12
a12=(rhov-rhol)*Vc;
%
%compute a21
a21=((1-alpha_c)*deriv(pssr,rhol_list.*Hl_list,pc,.01)+...
alpha_c*(deriv(pssr,rhov_list.*Hv_list,pc,.01))-1)*Vc;
%
%compute a22
a22=(rhov*Hv - rhol*Hl)*Vc;
%
%compute a33
a33=Dt/2*Lt*rhol*(sin(acos(1-2*hl/Dt)))^2/sqrt(hl/Dt*(1-hl/D
t));
%
%complete A
A=[a11,a12,0;a21,a22,0;0,0,a33];
end
```

```
function y = deriv(x,y,input,delta)
%
%computes the derivative of y wrt x at the input value of x,
%using an x step
%of delta
%format is y = deriv(x,y,input,delta)
y = (spline(x,y,input+delta)-spline(x,y,input))/delta;

end
```

```
function [hl,hv,Tsat,mu,k,rho_v,rho_l] = stminfo (p)
%
%function to compute the properties of water given pressure
%
%for pressure in the range 1.5MPa to 9Mpa
%
%function [hl,hv,Tsat,mu,k,rho_v,rho_l] = stminfo (p)

k=626e-6;%thermal conductivity
%steam table information
press = [1.5e6;2e6;2.5e6;3e6;3.5e6;4e6;4.5e6;5e6;5.5e6;...
6e6;6.5e6;7e6;7.5e6;8e6;8.5e6;9e6];

rhol=[866.6262;849.9065;835.4219;822.1656;810.0446;...
798.6583;787.9600;777.7259;767.8722;758.3226;749.0637;...
740.0281;731.1545;722.4390;713.7759;705.2684];

rhov = [7.5953;10.0462; 12.6855; 15.0083; 17.5346;...
20.1005; 22.7066; 25.3614; 28.0662; 30.8261; 33.6485;...
 36.5323; 39.4836; 42.5080; 45.4339; 48.7924];

Hl=1.0e+03*[.8447;0.9086;0.9618;1.0084;1.0498;1.0874;...
1.1221;1.1545;1.1849;1.2137;1.2417;1.2674;1.2927;1.3171;...
1.3404;1.3637];
Hv=1.0e+03*[2.7899;2.7972;2.8009;2.8023;2.8020;2.8003;...
2.7977;2.7942;2.7899;2.7850;2.7795;2.7735;2.7669;2.7599;...
2.7523;2.7446];
TSAT = [198.29;212.37;223.91;233.84;242.54;250.33;257.41;...
263.91;269.93;275.55;280.82;285.79;290.5;294.97;299.14;303.3
1];
%interpolate to get precise T and P in generator for given
power %level
%i and i+1 are the indices in the list that bracket the
value %sought
i=comp(p,press);
if i==length(press)
  rho_v=rhov(i);
  rho_l=rhol(i);
  hv=Hv(i);
  hl=Hl(i);
  Tsat=TSAT(i);
else
  rho_v=(p-press(i))./(press(i+1)-press(i)).*(rhov(i+1)-...
rhov(i))+rhov(i);
  rho_l=(p-press(i))./(press(i+1)-press(i)).*(rhol(i+1)-...
rhol(i))+rhol(i);

hv=(p-press(i))./(press(i+1)-press(i)).*(Hv(i+1)-Hv(i))+...
Hv(i);

hl=(p-press(i))./(press(i+1)-press(i)).*(Hl(i+1)-Hl(i))+...
Hl(i);
```

```
  Tsat=(p-press(i))./(press(i+1)-press(i)).*(TSAT(i+1)-...
TSAT(i))+TSAT(i);
end
mu=visc(Tsat,rho_l);
end
```

```
function [index]=comp(value,list)
%function index=compare(value,list)
%function that compares each element of value with all the
values in a
%sorted list and returns the a vector containing the index
of the closest
%number below each element of value in list

index=zeros(1,length(value));
for j=1:length(value);
    for i=1:length(list);
      if value(j)>=list(i)
        index(j)=i;
      end
    end
    if index(j)==0
      disp('')
    disp('number is not in given range')
    end
end
end
```

```
function [Q]=findQ(p)
%function to compute heat transfer rate as a function of
pssr in %condensing pot
%function [Q]=findQ(p)

%constants
g=9.807;
Tamb=50;
%wtd length.  length is 3.5 inches half of which is 1.75
inches=5.08e-2
l=3.5/2*2.54e-2;
%l=3.81e-2;
%rin=7.42e-2;
%rout=7.62e-2;
rin=1.939*2.54e-2/2;%based on sched 80, 2 in diameter
rout=2.157*2.54e-2/2;
ksteel=50;
hout=11;
%
%get steam data
[hl,hv,Tsat,mu,k,rho_v,rho_l]=stminfo(p);
%
%hfg=hv-hl;
%compute hbar
%Nu=(hfg.*rho_l.^2*g*l^3./(4*mu*k.*(Tsat-Tsurf))).^.25;
%hbar=4/3*k*1e3/l*Nu;%1e3 needed since k is in kW
%compute UA
%UA=((1/(2*pi*rin*l*hbar))+(log(rout/rin)/(2*pi*l*ksteel))+.
..
(1/(2*pi*rout*l*...
%hout)))^(-1);
UA=((log(rout/rin)/(2*pi*l*ksteel))+(1/(2*pi*rout*l*...
hout)))^(-1);
%compute Q
Q=UA.*(Tsat-Tamb);%mass flow rate
end
```

```
function [mdotw] = findmdot(alpha_c,Dc,Dt,pc,theta)
%
%function to compute the mass flow rate in the weir
%
%alpha_c is the vapor volume fraction in the condensing pot
%Dc is the diameter of the condensing pot
%Dt is the diameter of the drain pipe
%pc is the pressure in the condensing pot
%theta is the elevation angle of the drain pipe
%
%uses:
%    1.stminfo.m
%    2.interp.m

%constants
g=9.807;
al=2;
%find the liquid density
[a,b,c,d,e,f,rhol] = stminfo (pc);
%find the phi_c that corresponds to the given alpha_c

phi_c=interp(alpha_c);%call special routine to find phi_c



hlc=Dc/2*(1-cos(phi_c));%liq ht in condensate pot
%
if hlc>(Dc-Dt)/2 & hlc<(Dc+Dt)/2 %make sure hlc in correct
range
  hw=hlc-(Dc-Dt)/2;
else
  hw=-1;%tube is plugged or empty
end
%
if hw~=-1 %tube not plugged
  phi_w = acos(1-2*hw/Dt);
  alpha_b = 1-(phi_w - sin(phi_w)*cos(phi_w))/pi;
else
  alpha_b = 1;
end
%alpha_b is the vapor volume fraction at the weir
%
%use eqn ()
mdotw =
rhol*(Dt/2)^2*pi*(1-alpha_b)*sqrt(g*Dt*cos(theta)/al);
end
```

```
function [phi_c]=interp(alpha_c)
%
%function [phi_c]=interp(alpha_c)
%
%function that finds phi given alpha using bisection search

phi_c=pi/2;
bottom=0;
top=pi;
diff=1;
while abs(diff)>5e-9,
diff=alpha_c-(1-(phi_c-sin(phi_c)*cos(phi_c))/pi);
if diff < 0
  bottom=phi_c;
  phi_c=phi_c+(top-phi_c)/2;
else
  top=phi_c;
  phi_c=phi_c-(phi_c-bottom)/2;
end
end
end
```

```
function [jl,jv]= findjvjl(hl,Pprime,h,press,jvdat,jldat)
%
%This macro does a 2 way interpolation on jv and jl data
compiled %as a function of both hl and P'
%hl is liquid height in the drain pipe
%Pprime is dP/dx for the tube
%press and givenh are the P' and h data used to compute the
jvdat %and jldat tables
%
%function [jl,jv]= findjvjl(hl,Pprime,h,press,jvdat,jldat)
%

%find out where hl and Pprime fall in the range of h's and
%press's available
%

%note that h and press contain all the possible values of hl
and %Pprime
%
a=find(hl<=h & hl>=h(1)); %first element of a is the first h
%higher than given hl
b=find(Pprime>=press & Pprime<=press(1));
%
%now select the 4 jv/jl values that bracket the hl and P'
given
%
if length(a)~=0 & length(b)~= 0 %hl and Pprime were in the
%correct ranges
%
%fix pressure index (at lower bracket value, one less than
b(1)
  if b(1)==1
    b_=1;      %in case pressure index already at lowest
%value,don't decrement
  else
    b_=b(1)-1;%fix pressure index at next lower value
  end
%drop hl index to lower bracket
  if a(1)==1
    a_=a(1)+1; %so a_-2 will be 0,not negative
  else
    a_=a(1);
  end
  jvh1=jvdat(41*(a_-2)+b_);%lower bracket hl and Pprime data
  jlh1=jldat(41*(a_-2)+b_);

%bump hl index back to upper bracket
  if b(1)==1
    b_=1;      %in case pressure index already at lowest
%value,don't decrement
  else
    b_=b(1)-1;%keep pressure index at next lower value
```

```
  end
  a_=a(1);
  jvh2=jvdat(41*(a_-1)+b_);%upper bracket h1, lower bracket
%Pprime data
  jlh2=jldat(41*(a_-1)+b_);

%bump pressure to upper bracket
%
%fix pressure index (at upper bracket)
  if b(1)==1
    f_=2;      %in case pressure index already at lowest
%value,bump up
  else
    f_=b(1);  %put pressure index at upper bracket
  end

%drop h1 index to lower bracket
  if a(1)==1
    g_=a(1)+1;
  else
    g_=a(1);
  end
  jvh3=jvdat(41*(g_-2)+f_);%lower bracket h1, upper bracket
P'
  jlh3=jldat(41*(g_-2)+f_);

%bump h1 index back to upper bracket
  if b(1)==1
    f_=2;      %in case pressure index already at lowest
%value,bump up
  else
    f_=b(1);  %put pressure index at upper bracket
  end
  g_=a(1);
  jvh4=jvdat(41*(g_-1)+f_);%upper bracket h1 and P'
  jlh4=jldat(41*(g_-1)+f_);
%  jvh4=jvdat(11*(g_-1)+f_);%upper bracket h1 and P'
%  jlh4=jldat(11*(g_-1)+f_);

%interpolate between h values
if a(1)==1
  h1=h(1);
else
  h1=h(a(1)-1);
end
h2=h(a(1));
h3=h1;
h4=h2;
%these if's are required since h1 might = h2 and the same
for h3 %and h4
if h2==h1
  jv5=jvh1;
```

```
else
  jv5=(h1-h1)./(h2-h1)*(jvh2-jvh1)+jvh1;
end
if h2==h1
  jv6=jvh3;
else
  jv6=(h1-h3)./(h4-h3)*(jvh4-jvh3)+jvh3;
end
if h2==h1
  jl5=jlh1;
else
  jl5=(h1-h1)./(h2-h1)*(jlh2-jlh1)+jlh1;
end
if h2==h1
  jl6=jlh3;
else
  jl6=(h1-h3)./(h4-h3)*(jlh4-jlh3)+jlh3;
end

%interpolate between 5 6 for Pprime
if b(1)==1
  p1=press(b(1));
else
  p1=press(b(1)-1);
end
if b(1)==1
  p2=press(b(1)+1);
else
  p2=press(b(1));
end

jv=(Pprime-p1)./(p2-p1)*(jv6-jv5)+jv5;
jl=(Pprime-p1)./(p2-p1)*(jl6-jl5)+jl5;

else
 b
 a
 disp('h1 and Pprime were not in the correct ranges for...
findjvjl.m')
end
end
```